Universität Regensburg
Mathematik

Parametric Approximation of Surface Clusters driven by Isotropic and Anisotropic Surface Energies

J.W. Barrett, H. Garcke, R. Nürnberg

Preprint Nr. 04/2009

Parametric Approximation of Surface Clusters driven by Isotropic and Anisotropic Surface Energies

John W. Barrett[†] Harald Garcke[‡] Robert Nürnberg[†]

Abstract

We present a variational formulation for the evolution of surface clusters in $\mathbb{R}^3$ by mean curvature flow, surface diffusion and their anisotropic variants. We introduce the triple junction line conditions that are induced by the considered gradient flows, and present weak formulations of these flows. In addition, we consider the case where a subset of the boundaries of these clusters are constrained to lie on an external boundary. These formulations lead to unconditionally stable, fully discrete, parametric finite element approximations. The resulting schemes have very good properties with respect to the distribution of mesh points and, if applicable, volume conservation. This is demonstrated by several numerical experiments, including isotropic double, triple and quadruple bubbles, as well as clusters evolving under anisotropic mean curvature flow and anisotropic surface diffusion, including for regularized crystalline surface energy densities.

Key words. surface clusters, mean curvature flow, surface diffusion, soap bubbles, triple junction lines, parametric finite elements, anisotropy, tangential movement

AMS subject classifications. 65M60, 65M12, 35K55, 53C44, 74E10, 74E15

1 Introduction

Equilibrium soap bubble clusters are stationary solutions of the variational problem in which one seeks a least area way to enclose and separate a number of regions with prescribed volumes. The relevant energy in this case is given as the sum of the total surface area. In this paper we study gradient flows of this energy leading to mean curvature flow and surface diffusion depending on whether we consider the gradient flow with respect to the L^2- or the H^{-1}-inner product. In the case of surface diffusion the enclosed volumes are preserved, and hence stationary solutions are soap bubble clusters; whereas in the case of mean curvature flow the enclosed volumes are not preserved, and bounded initial data will in general vanish in finite time.

[†]Department of Mathematics, Imperial College London, London, SW7 2AZ, UK
[‡]NWF I – Mathematik, Universität Regensburg, 93040 Regensburg, Germany

For the above geometric flows one has to impose angle conditions at points where different surfaces meet, or where a surface meets a fixed external boundary. For example, in the case of mean curvature flow with equal constant surface energy densities a 120° angle condition has to hold at triple junction lines, while a 90° contact angle holds where a surface meets an external boundary. Mean curvature flow is a parabolic equation of second order, whereas surface diffusion leads to a parabolic equation of fourth order. As surface diffusion is of higher order, one would expect that additional boundary conditions have to hold at triple junction and boundary contact lines. Physically motivated boundary conditions have been derived by Garcke and Novick-Cohen (2000), via formal asymptotics, as a singular limit of a degenerate Cahn–Hilliard system. It turns out that, besides the angle condition, a flux condition and, in the case of triple junction lines, a condition related to the continuity of the chemical potentials have to be prescribed. Geometrically the triple junction line conditions imply that the derivatives of the mean curvature in the direction of the conormal of the surfaces are equal and that a weighted sum of the mean curvatures of the surfaces has to vanish, respectively. The last condition is also related to the well-known fact that for an equilibrium soap bubble cluster the mean curvature of the surface is given as a pressure difference. This, together with the fact that the flow is volume preserving, is the reason why steady state solutions for surface diffusion with triple junction lines are natural candidates for surface area minimizing soap bubble constellations for fixed given volumes. Intriguingly, although the search for such area minimizing constellations historically has received a lot of attention among mathematicians, only very few things are actually known. For instance, for two enclosed volumes it is known that the so-called standard double bubble is the unique global minimizer, see Hutchings *et al.* (2002). We refer to the recent review article Morgan (2007) for more details on historical developments and open questions in this area.

In the plane existence of solutions for mean curvature flow and surface diffusion with triple junction points has been shown by Bronsard and Reitich (1993) and Garcke and Novick-Cohen (2000), respectively. For the higher dimensional case it is known that very weak solutions exist for the mean curvature flow. In fact, the theory of Brakke, who in his seminal paper Brakke (1978) first proved an existence result for the mean curvature flow of so-called varifolds of arbitrary dimension and codimension, also allows one to consider triple junctions. A well-posedness result for classical solutions of the mean curvature flow of surface clusters in $\mathbb{R}^3$ has been shown recently by Depner *et al.* (2009). To the best of our knowledge, corresponding results for the surface diffusion flow of surface clusters with triple junction lines remain open.

Here we will also study situations in which the energy is proportional to surface area, but now the constant of proportionality might be different on each of the surfaces making up the bubble. This frequently appears in the case of clusters of immiscible fluids, where the energy depends upon which fluids are separated by the surface. Another important situation in applications is the case when the surface energy depends not only on its area but also on its tangent plane (which for hypersurfaces is equivalent to a dependence on the normal). Such energies are called anisotropic, and for highly anisotropic situations equilibrium shapes can be polytopes. In such a case one speaks of crystalline energies. For a good introduction to variational problems involving clusters we refer to the book

Morgan (1988), where also the most relevant references can be found. In addition, we refer to Almgren (1976); Taylor (1976); Foisy *et al.* (1993); Lawlor and Morgan (1994); Morgan (1994); Hass *et al.* (1995); Almgren and Taylor (1996); Sullivan and Morgan (1996); Taylor (1999) for additional information on variational problems involving surface energies for clusters. Curvature driven surface evolution with triple junction lines and/or boundary contact plays a fundamental role in many applications. For example, grain boundaries are driven by mean curvature flow and surface diffusion is an important transport mechanism in the context of thermal grooving, epitaxial growth and electromigration, see e.g. Smith (1948); Herring (1951); Mullins (1956); Sutton and Balluffi (1995) and the references therein.

In this paper we study the evolution of surface clusters by mean curvature flow or surface diffusion, and their anisotropic variants, in $\mathbb{R}^3$. In particular, we are interested in the numerical approximation of these geometric evolution laws for surface clusters. This paper generalizes the parametric finite element approximation for the evolution of curve networks in the plane, that was introduced and analysed by the present authors in Barrett, Garcke, and Nürnberg (2007a,b, 2008a), to the natural analogue in three space dimensions. Of course, in this higher dimensional setting the topology is richer, and, in addition to triple junction lines, quadruple junction points have to be considered. In particular, we will present parametric finite element approximations for second and fourth order geometric evolution equations that are unconditionally stable and that exhibit very good mesh properties. The latter makes a heuristical remeshing during the evolution unnecessary. Finally, we will also extend these approximations from isotropic to anisotropic surface energy densities, on utilizing ideas that were introduced by the present authors in Barrett, Garcke, and Nürnberg (2008c).

Existing approaches for the numerical approximation of surface clusters include the well-known Surface Evolver by Brakke, Brakke (1992), where a direct parameterization and a gradient descent method for a given energy are used in order to find certain surface area minimizers. We note that the Surface Evolver has recently been used to numerically study large soap bubble clusters, see e.g. Cox and Graner (2004) and Kraynik *et al.* (2004). A level set approach for the simulation of the evolution of soap bubbles has been considered in Zhao *et al.* (1998). Phase field methods can be used to approximate curvature flows with triple junction lines and we refer to, e.g. Garcke *et al.* (2008) and Nestler *et al.* (2008). Numerical results for a finite element approximation of a phase field model for multi-component surface diffusion, i.e. surface diffusion with triple junction lines, are given in Nürnberg (2009); while an alternative finite element approximation of the same phase field model will be given in the forthcoming article Barrett, Garcke, and Nürnberg (2009). Note that most of the existing numerical results are for isotropic surface energies only.

Let us now specify the geometric evolution equations for a cluster of surfaces in more detail. We assume that the surface cluster is connected and consists of $I_S \in \mathbb{N}$, $I_S \geq 3$, hypersurfaces with boundaries in $\mathbb{R}^3$, and $I_T \in \mathbb{N}$, $I_T \geq 0$, different triple junction lines. In order to parameterize the surfaces we choose a collection of domains $\Omega_i \subset \mathbb{R}^2$, $i = 1 \to I_S$. The surface cluster is then given with the help of parameterizations $\vec{x}_i : \Omega_i \times [0,T] \to \mathbb{R}^3$

with $\vec{x}_i(\Omega_i,t)=\Gamma_i(t)$, where the Γ_i, $i=1\to I_S$, are the surfaces constituting the cluster. Here and throughout we will often use the shorthand notation $\vec{x}(\Omega,t)=\Gamma(t)$, where $\Omega:=(\Omega_1,\ldots,\Omega_{I_S})$ and $\Gamma(t):=(\Gamma_1(t),\ldots,\Gamma_{I_S}(t))$. Note that for the standard double bubble we have that $I_S=3$ with $I_T=1$, and for the standard triple bubble we have that $I_S=6$ and $I_T=4$, see e.g. Figures 4 and 11. In the former case two volumes are enclosed by the surface cluster, in the latter three. In these cases, one can choose, for example, all the domains Ω_i, $i=1\to I_S$, as the unit disk in $\mathbb{R}^2$; $\Omega_i=\{\vec{z}\in\mathbb{R}^2:|\vec{z}|\leq 1\}$ with boundary $\partial\Omega_i=S^1$, i.e. the unit circle in $\mathbb{R}^2$.

Typically three surfaces meet at line junctions, and in this paper we will restrict ourselves to this case; i.e. we will not allow for four surfaces meeting at a line. In the case that all surfaces have the same isotropic energy such a case would be unstable. But we point out that quadruple junction lines can also be stable, if the energies are not the same; see e.g. Cahn *et al.* (1992) and Garcke *et al.* (1999). Fundamental for the following considerations will be the identities

$$\Delta_s\,\vec{x}_i=\vec{\varkappa}_i\equiv\varkappa_i\,\vec{\nu}_i\,,\qquad i=1\to I_S\,, \tag{1.1}$$

which for a single surface, with or without boundary, was first used by Dziuk (1991) to design a finite element method for geometric partial differential equations and mean curvature flow; see also Dziuk (1994). The identity (1.1) is well-known from surface geometry, see e.g. Deckelnick, Dziuk, and Elliott (2003), where ∇_s is the surface (tangential) gradient, $\Delta_s\equiv\nabla_s\,.\,\nabla_s$ is the surface Laplacian (Laplace–Beltrami operator), $\vec{x}_i$ is a parameterization of Γ_i, $\vec{\varkappa}_i$ is the mean curvature vector, $\varkappa_i$ is the sum of the principal curvatures and $\vec{\nu}_i$ is a unit normal to Γ_i. Here we use the sign convention that $\varkappa_i$ is positive, if the surface Γ_i is curved in the direction of the normal $\vec{\nu}_i$. In this paper, we will investigate the motion of the surface cluster by mean curvature flow

$$\mathcal{V}_i=\varkappa_i\,,\qquad i=1\to I_S, \tag{1.2}$$

where $\mathcal{V}_i:=[\vec{x}_i]_t\,.\,\vec{\nu}_i$ is the normal velocity of the surface Γ_i; and the motion by surface diffusion

$$\mathcal{V}_i=-\Delta_s\,\varkappa_i\,,\qquad i=1\to I_S\,. \tag{1.3}$$

In addition to the above differential equations, certain boundary conditions have to be prescribed at the boundaries of the surfaces Γ_i, $i=1\to I_S$, and this will be outlined below. We remark that it is also possible to consider a setup, where motion by mean curvature is only prescribed for a subset of the surfaces making up the cluster, while the remaining surfaces move by motion by surface diffusion. This is of relevance e.g. in thermal grooving (Mullins (1958)), in interface motion in polycrystalline two-phase materials (Cahn (1991)), and in the evolution of boundaries in the electromigration of intergranular voids (see Barrett, Garcke, and Nürnberg (2007c)). A parametric finite element approximation of such flows for curve networks in the plane has been considered in Barrett, Garcke, and Nürnberg (2007b). However, in this paper we will only consider the purely second and fourth order flows (1.2) and (1.3), respectively, as well as their anisotropic counterparts.

In order to describe the necessary conditions that need to hold at triple junction lines, where three surfaces meet, and at quadruple junction points, where four triple

junction lines meet, we introduce the following notation. Assume that $\partial\Omega_i$, the boundary of Ω_i, is partitioned into $\partial_j\Omega_i$, $j = 1 \to I_P^i$, $I_P^i \geq 1$. Then the triple junction lines $\mathcal{T}_k$, $k = 1 \to I_T$, are parameterized with the help of the partitioned boundaries $\partial_j\Omega_i$, $j = 1 \to I_P^i$, $i = 1 \to I_S$. We assume that for each $\mathcal{T}_k$, there exist pairs (s_1^k, p_1^k), (s_2^k, p_2^k) and (s_3^k, p_3^k) with $s_1^k < s_2^k < s_3^k$, such that

$$\mathcal{T}_k(t) := \vec{x}_{s_1^k}(\partial_{p_1^k}\Omega_{s_1^k}, t) = \vec{x}_{s_2^k}(\partial_{p_2^k}\Omega_{s_2^k}, t) = \vec{x}_{s_3^k}(\partial_{p_3^k}\Omega_{s_3^k}, t)\,, \qquad k = 1 \to I_T\,. \tag{1.4a}$$

Note that for a standard double bubble, as in e.g. Figure 4, we simply have $I_T = I_P^i = 1$, $i = 1 \to 3$, and $\mathcal{T}_1$ is defined via $\big((s_j^1, p_j^1)\big)_{j=1}^3 = ((1,1),(2,1),(3,1))$. For a standard triple bubble, as in e.g. Figure 11, on the other hand, we have that $I_T = 4$ and $I_P^i = 2$, $i = 1 \to 6$, meaning that there are four triple junction lines and that the boundary of each surface Γ_i, $i = 1 \to 6$, partitions into two parts, each meeting a different triple junction line. The conditions that need to hold at a triple junction line, see e.g. Bronsard *et al.* (1998) and Garcke and Novick-Cohen (2000), can then be formulated as follows. In the case of mean curvature flow with isotropic and equal surface energies we require, in addition to the attachment conditions (1.4a), that

$$\sum_{j=1}^{3} \vec{\mu}_{s_j^k} = \vec{0} \quad \text{on } \mathcal{T}_k\,, \qquad k = 1 \to I_T, \tag{1.4b}$$

where $\vec{\mu}_i$ denotes the conormal, i.e. the intrinsic outer unit normal to $\partial\Gamma_i$, the boundary of Γ_i, that lies within the tangent plane of Γ_i. The identities (1.4b) are force balance conditions on the triple junction lines $\mathcal{T}_k \subset \mathbb{R}^3$, $k = 1 \to I_T$. In the case of equal isotropic energies, as considered here, the conditions (1.4b) lead to the well known 120° angle condition at triple junction lines. As mentioned above, we need additional boundary conditions for surface diffusion. To formulate these conditions we need to choose an appropriate orientation of the normals along the triple junction lines. Let $\vec{\nu}_i$ be a global normal field on Γ_i. Then we choose at a triple junction point on $\mathcal{T}_k$, $k = 1 \to I_T$, an orientation $o^k := (o_1^k, o_2^k, o_3^k)$, where $o_j^k \in \{-1, 1\}$, such that $(o_j^k\, \vec{\nu}_{s_j^k}, \vec{\mu}_{s_j^k})$, $j = 1 \to 3$, all have the same orientation in the plane orthogonal to $\mathcal{T}_k$ at that point; see Figure 1. Then the additional boundary conditions are

$$o_1^k\, \vec{\mu}_{s_1^k} \,.\, \nabla_s\, \varkappa_{s_1^k} = o_2^k\, \vec{\mu}_{s_2^k} \,.\, \nabla_s\, \varkappa_{s_2^k} = o_3^k\, \vec{\mu}_{s_3^k} \,.\, \nabla_s\, \varkappa_{s_3^k} \quad \text{on } \mathcal{T}_k\,, \qquad k = 1 \to I_T, \tag{1.4c}$$

$$\sum_{j=1}^{3} o_j^k\, \varkappa_{s_j^k} = 0 \quad \text{on } \mathcal{T}_k\,, \qquad k = 1 \to I_T; \tag{1.4d}$$

where (1.4c) are flux balance conditions and (1.4d) are chemical potential continuity conditions that need to hold on triple junction lines.

We remark that at quadruple junction points no extra conditions need to be prescribed, since the behaviour at quadruple junction points is completely determined by the triple junction line conditions; see Taylor (1976) or Bronsard *et al.* (1998) for details. In particular, as a consequence of the 120° degree angle conditions on the triple junction lines, at a quadruple junction the four triple junction curves meet at equal $\arccos(-\frac{1}{3})$

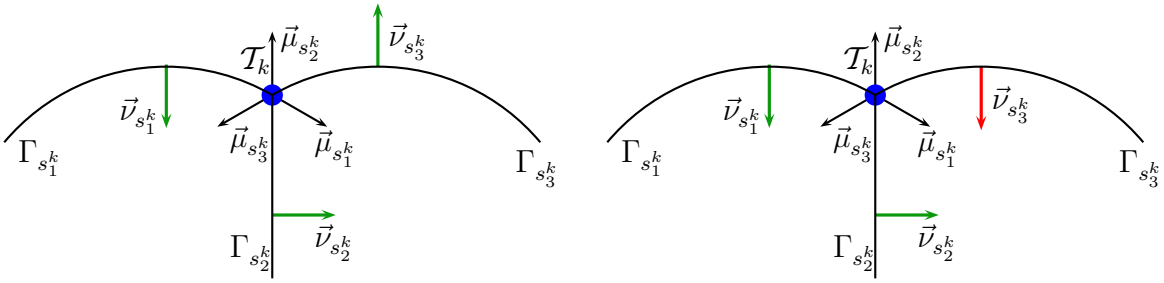

Figure 1: Sketch of the local orientation of $(\Gamma_{s_1^k}, \Gamma_{s_2^k}, \Gamma_{s_3^k})$ at the triple junction line $\mathcal{T}_k$ (**blue**). Depicted above is a plane T_k that is perpendicular to $\mathcal{T}_k$. In the example on the left, $o^k := (o_1^k, o_2^k, o_3^k)$ can be chosen as $o^k = (1,1,1)$. However, in the example on the right we require $o^k = \pm(1,1,-1)$.

angles, where $\arccos(-\frac{1}{3}) \approx 109^\circ$. We note that these angles are well-known in the theory of minimal surfaces, see e.g. Hildebrandt and Tromba (1985).

In conclusion, motion by mean curvature is given by (1.2) together with (1.4a,b), and surface diffusion is given by (1.3) with (1.4a–d). In Section 2 we show that both of these geometric evolution equations are gradient flows of the total surface area

$$E(\Gamma) = |\Gamma| := \sum_{i=1}^{I_S} \int_{\Gamma_i} 1 \,\mathrm{d}\mathcal{H}^2 \,, \tag{1.5}$$

where $\mathcal{H}^d$ is the d-dimensional Hausdorff measure in $\mathbb{R}^3$. In addition, the surface diffusion flow is volume preserving, i.e. the volume of each enclosed bubble is preserved; see Remark 2.1 below.

We now introduce weak formulations of these evolution equations. These weak formulations will form the basis of our finite element approximations, which we introduce in Section 3. Let $\widehat{W}(\Gamma) := \bigtimes_{i=1}^{I_S} H^1(\Gamma_i, \mathbb{R}) = \{(\chi_1, \ldots, \chi_{I_S}) : \chi_i \in H^1(\Gamma_i, \mathbb{R}),\ i = 1 \to I_S\}$ and

$$\underline{V}(\Gamma) := \{(\vec{\chi}_1, \ldots, \vec{\chi}_{I_S}) \in \bigtimes_{i=1}^{I_S} H^1(\Gamma_i, \mathbb{R}^3) : \vec{\chi}_{s_1^k} = \vec{\chi}_{s_2^k} = \vec{\chi}_{s_3^k} \ \text{ on } \mathcal{T}_k, \quad k = 1 \to I_T\} \,, \tag{1.6a}$$

$$W(\Gamma) := \{(\chi_1, \ldots, \chi_{I_S}) \in \widehat{W}(\Gamma) : \sum_{j=1}^{3} o_j^k \, \chi_{s_j^k} = 0 \ \text{ on } \mathcal{T}_k, \quad k = 1 \to I_T\} \,, \tag{1.6b}$$

where here and throughout $\Gamma = (\Gamma_1, \ldots, \Gamma_{I_S})$ with $\Gamma_i = \Gamma_i(t) = \vec{x}_i(\Omega_i, t)$, $i = 1 \to I_S$; where $\vec{x}(\cdot, t) \in \underline{V}(\Omega)$,

$$\underline{V}(\Omega) := \{(\vec{\chi}_1, \ldots, \vec{\chi}_{I_S}) \in \bigtimes_{i=1}^{I_S} H^1(\Omega_i, \mathbb{R}^3) : \vec{\chi}_{s_1^k}(\partial_{p_1^k}\Omega_{s_1^k}) = \vec{\chi}_{s_2^k}(\partial_{p_2^k}\Omega_{s_2^k}) = \vec{\chi}_{s_3^k}(\partial_{p_3^k}\Omega_{s_3^k}) \,, \quad k = 1 \to I_T\}. \tag{1.6c}$$

From now on, and throughout this paper, we will use the shorthand notation $\eta \in W(\Gamma)$ to mean $\eta = (\eta_1, \ldots, \eta_{I_S}) \in W(\Gamma)$, and similarly for other functions and quantities defined on all surfaces Γ_i, $i = 1 \to I_S$. In addition, for scalar, vector and tensor valued functions

$\eta,\, \chi \in \overset{I_S}{\underset{i=1}{\times}} L^2(\Gamma_i, Y)$, with $Y = \mathbb{R}$, $\mathbb{R}^3$ or $\mathbb{R}^{3\times 3}$, we define the L^2 inner product $\langle \cdot, \cdot \rangle$ over Γ as follows

$$\langle \eta, \chi \rangle := \sum_{i=1}^{I_S} \int_{\Gamma_i} \eta_i \cdot \chi_i \, \mathrm{d}\mathcal{H}^2 \,. \tag{1.7}$$

Following Barrett, Garcke, and Nürnberg (2007b, 2008b), we reformulate (1.2) and (1.3) as

$$[\vec{x}_i]_t \,.\, \vec{\nu}_i = \varkappa_i \,, \qquad \varkappa_i \, \vec{\nu}_i = \Delta_s \, \vec{x}_i \,, \qquad i = 1 \to I_S \,, \tag{1.8}$$

$$\text{and} \qquad [\vec{x}_i]_t \,.\, \vec{\nu}_i = -\Delta_s \, \varkappa_i \,, \qquad \varkappa_i \, \vec{\nu}_i = \Delta_s \, \vec{x}_i \,, \qquad i = 1 \to I_S \,; \tag{1.9}$$

respectively. Then multiplying the first equation in (1.8) with a test function $\eta \in \widehat{W}(\Gamma)$ and the second equation with a test function $\vec{\chi} \in \underline{V}(\Gamma)$, integrating over Γ and using Green's formula for surfaces, we obtain the following weak formulation for mean curvature flow: Find $\vec{x} \in \underline{V}(\Omega)$ and $\varkappa \in \widehat{W}(\Gamma)$ such that

$$\langle \vec{x}_t, \eta \, \vec{\nu} \rangle - \langle \varkappa, \eta \rangle = 0 \qquad \forall \; \eta \in \widehat{W}(\Gamma) \,, \tag{1.10a}$$

$$\langle \varkappa \, \vec{\nu}, \vec{\chi} \rangle + \langle \nabla_s \, \vec{x}, \nabla_s \, \vec{\chi} \rangle = 0 \qquad \forall \; \vec{\chi} \in \underline{V}(\Gamma) \,. \tag{1.10b}$$

Similarly, for the surface diffusion flow we obtain: Find $\vec{x} \in \underline{V}(\Omega)$ and $\varkappa \in W(\Gamma)$ such that

$$\langle \vec{x}_t, \eta \, \vec{\nu} \rangle - \langle \nabla_s \, \varkappa, \nabla_s \, \eta \rangle = 0 \qquad \forall \; \eta \in W(\Gamma) \,, \tag{1.11a}$$

$$\langle \varkappa \, \vec{\nu}, \vec{\chi} \rangle + \langle \nabla_s \, \vec{x}, \nabla_s \, \vec{\chi} \rangle = 0 \qquad \forall \; \vec{\chi} \in \underline{V}(\Gamma) \,. \tag{1.11b}$$

We observe that in the above the conditions (1.4b), and where applicable (1.4c), are formulated weakly, while the remaining conditions are enforced strongly through the trial spaces; recall (1.6a,b).

In the remainder of this section, we outline the generalizations of (1.10a,b) and (1.11a,b) to the case of fully anisotropic surface energies. In this case the isotropic free energy (1.5) is replaced by the anisotropic energy

$$E_\gamma(\Gamma) = |\Gamma|_\gamma := \sum_{i=1}^{I_S} |\Gamma_i|_{\gamma_i} := \sum_{i=1}^{I_S} \int_{\Gamma_i} \gamma_i(\vec{\nu}_i) \, \mathrm{d}\mathcal{H}^2 \,, \tag{1.12}$$

where $\gamma := (\gamma_1, \ldots, \gamma_{I_S})$ with γ_i, $i = 1 \to I_S$, being positive and absolutely homogeneous functions of degree one; i.e. in particular $\gamma_i : \mathbb{R}^3 \to \mathbb{R}_{\geq 0}$ with $\gamma_i(\vec{p}) > 0$ if $\vec{p} \neq \vec{0}$ and

$$\gamma_i(\lambda \, \vec{p}) = |\lambda| \, \gamma_i(\vec{p}) \quad \forall \; \vec{p} \in \mathbb{R}^3, \; \forall \; \lambda \in \mathbb{R} \quad \Rightarrow \quad \gamma_i'(\vec{p}) \,.\, \vec{p} = \gamma_i(\vec{p}) \quad \forall \; \vec{p} \in \mathbb{R}^3 \setminus \{\vec{0}\}, \tag{1.13}$$

where γ_i' is the gradient of γ_i. In the isotropic case we have that

$$\gamma_i(\vec{p}) = \sigma_i \, |\vec{p}| \,, \quad \text{with} \;\; \sigma_i > 0 \,, \qquad i = 1 \to I_S, \tag{1.14}$$

which implies that $\gamma_i(\vec{\nu}) = \sigma_i$; and so $|\Gamma_i|_{\gamma_i}$ in (1.12) reduces to $\sigma_i \, |\Gamma_i|$, the scaled surface area of Γ_i. In the isotropic equal energy density case we have, in addition, that $\sigma_i = 1$, $i = 1 \to I_S$; and so $E_\gamma(\Gamma)$ reduces to $E(\Gamma)$, the surface area of Γ.

Following our recent work in Barrett, Garcke, and Nürnberg (2008a,c), we will restrict ourselves to anisotropic surface energy densities of the form

$$\gamma_i(\vec{p}) = \left(\sum_{\ell=1}^{L_i} [\gamma_i^{(\ell)}(\vec{p})]^{r_i} \right)^{\frac{1}{r_i}}, \qquad \text{where} \qquad \gamma_i^{(\ell)}(\vec{p}) := \sqrt{\vec{p}\,.\, G_i^{(\ell)}\,\vec{p}},$$

$$\Rightarrow \qquad \gamma_i'(\vec{p}) = [\gamma_i(\vec{p})]^{1-r_i} \sum_{\ell=1}^{L_i} [\gamma_i^{(\ell)}(\vec{p})]^{r_i-1}\, [\gamma_i^{(\ell)}]'(\vec{p})\,, \tag{1.15}$$

where $r_i \in [1,\infty)$ and $G_i^{(\ell)} \in \mathbb{R}^{3\times 3}$, $\ell = 1 \to L_i$, are symmetric and positive definite; $i = 1 \to I_S$. This class of convex anisotropies (1.15) will lead to unconditionally stable numerical approximations, see Section 3 below.

In order to visualize some anisotropies of the form (1.15), we briefly recall the definition of the Wulff shape. For a given anisotropy function γ_i one defines its Frank diagram

$$\mathcal{F}_i := \{\vec{p} \in \mathbb{R}^3 : \gamma_i(\vec{p}) \leq 1\}$$

and the corresponding Wulff shape, Wulff (1901),

$$\mathcal{W}_i := \{\vec{q} \in \mathbb{R}^3 : \gamma_i^*(\vec{q}) \leq 1\}\,, \quad \text{where} \quad \gamma_i^*(\vec{q}) := \sup_{\vec{p}\in\mathbb{R}^3\setminus\{\vec{0}\}} \frac{\vec{p}\,.\,\vec{q}}{\gamma_i(\vec{p})}\,. \tag{1.16}$$

As the Wulff shape $\mathcal{W}_i$ is known to be the solution of an isoperimetric problem, i.e. the boundary of $\mathcal{W}_i$ is the minimizer of $|\cdot|_{\gamma_i}$ in the class of all (closed) surfaces enclosing the same volume, see e.g. Fonseca and Müller (1991), it can be used to visualize the given anisotropy. In Figures 2 and 3 we give the Frank diagrams and Wulff shapes for some anisotropies γ_i of the form (1.15); most of which have already been considered in Barrett, Garcke, and Nürnberg (2008c). Here we briefly state their definitions. Let

$$G_i^{(\ell)} := R(\vec{\theta}_i^{(\ell)})^T \,\mathrm{diag}(1,\varepsilon_i^2,\varepsilon_i^2)\, R(\vec{\theta}_i^{(\ell)})\,, \tag{1.17}$$

where $\mathrm{diag}(a,b,c)$ denotes a diagonal matrix with diagonal entries a,b,c and $R(\vec{\theta}) := R_1(\theta_1)\, R_2(\theta_2)\, R_3(\theta_3)$ with

$$R_1(\theta) := \begin{pmatrix} \cos\theta & \sin\theta & 0 \\ -\sin\theta & \cos\theta & 0 \\ 0 & 0 & 1 \end{pmatrix},\ R_2(\theta) := \begin{pmatrix} \cos\theta & 0 & \sin\theta \\ 0 & 1 & 0 \\ -\sin\theta & 0 & \cos\theta \end{pmatrix} \text{ and } R_3(\theta) := \begin{pmatrix} 1 & 0 & 0 \\ 0 & \cos\theta & \sin\theta \\ 0 & -\sin\theta & \cos\theta \end{pmatrix}$$

being rotation matrices through the given angle θ. For the anisotropies in Figure 2 we used $r_i = 1$ and $\varepsilon_i = 10^{-2}$ with $(\vec{\theta}_i^{(1)},\dots,\vec{\theta}_i^{(L_i)}) = (\vec{0},(\frac{\pi}{2},0,0),(0,\frac{\pi}{2},0))$ and $(\vec{0},(0,\frac{\pi}{3},0),(0,\frac{2\pi}{3},0),(\frac{\pi}{2},0,0))$, respectively. Using the former example but now setting $r_i = 30$ yields the Frank diagram and Wulff shape as on the left of Figure 3. The final displayed anisotropy in Figure 3 can be obtained by choosing $r_i = 30$ and, for (1.17), setting $\varepsilon_i = 10^{-2}$ and $(\vec{\theta}_i^{(1)},\dots,\vec{\theta}_i^{(L_i)}) = (\vec{0},(0,\frac{\pi}{2},0),(\frac{\pi}{4},0,0),(-\frac{\pi}{4},0,0),(0,\frac{\pi}{2},\frac{\pi}{4}),(0,\frac{\pi}{2},-\frac{\pi}{4}))$.

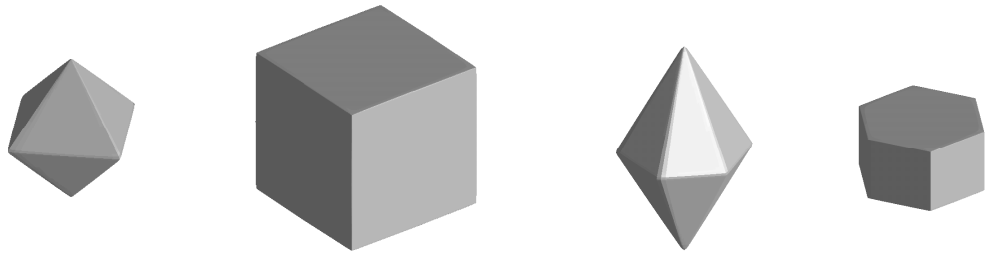

Figure 2: Frank diagrams and Wulff shapes for different choices of (1.15) with $L_i = 3, 4$, $r_i = 1$.

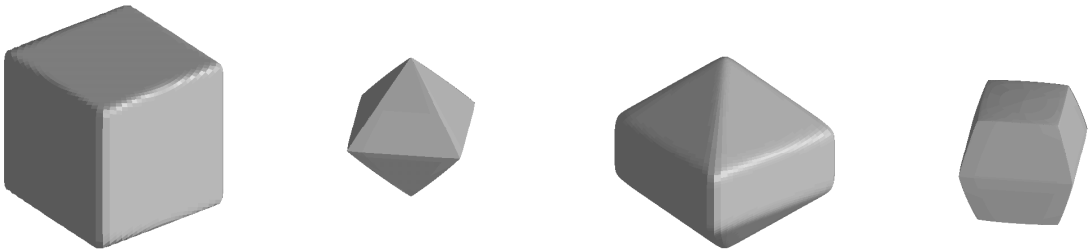

Figure 3: Frank diagrams and Wulff shapes for different choices of (1.15) with $L_i = 3, 6$ and $r_i = 30$.

In order to define anisotropic mean curvature flow and anisotropic surface diffusion, we introduce the Cahn–Hoffmann vectors, see Cahn and Hoffmann (1974),

$$\vec{\nu}_{\gamma,i} := \gamma_i'(\vec{\nu}_i)\,, \qquad i = 1 \to I_S\,; \tag{1.18a}$$

and define the weighted mean curvatures as

$$\varkappa_{\gamma,i} := -\nabla_s\,.\,\vec{\nu}_{\gamma,i} \qquad i = 1 \to I_S\,. \tag{1.18b}$$

Then the anisotropic versions of mean curvature flow, (1.2), and surface diffusion, (1.3), are given by

$$\mathcal{V}_i = \beta_i(\vec{\nu}_i)\,\varkappa_{\gamma,i}\,, \qquad i = 1 \to I_S\,, \tag{1.19}$$

and

$$\mathcal{V}_i = -\nabla_s\,.\,(\beta_i(\vec{\nu}_i)\,\nabla_s\,\varkappa_{\gamma,i})\,, \qquad i = 1 \to I_S\,; \tag{1.20}$$

where $\beta_i : S^2 \to \mathbb{R}_{>0}$, $i = 1 \to I_S$, are kinetic coefficients, and are assumed to be smooth, even and positive functions defined on the unit sphere $S^2 \subset \mathbb{R}^3$. For a derivation of these laws in the case of a single closed hypersurface we refer to Angenent and Gurtin (1989); Gurtin (1993); Taylor *et al.* (1992); Taylor and Cahn (1994).

Naturally, the triple junction line conditions (1.4a–d) need to be generalized to the anisotropic setting. Of course, the attachment conditions (1.4a) still need to hold. In

addition, the following conditions have to hold on the triple junction lines:

$$\sum_{j=1}^{3} \left[\gamma_{s_j^k}(\vec{\nu}_{s_j^k})\, \vec{\mu}_{s_j^k} - (\gamma'_{s_j^k}(\vec{\nu}_{s_j^k}) \,.\, \vec{\mu}_{s_j^k})\, \vec{\nu}_{s_j^k} \right] = \vec{0} \quad \text{on } \mathcal{T}_k\,, \quad k = 1 \to I_T, \tag{1.21a}$$

$$o_1^k\, \vec{\mu}_{s_1^k} \,.\, \beta_{s_1^k}(\vec{\nu}_{s_1^k})\, \nabla_s\, \varkappa_{\gamma,s_1^k} = o_2^k\, \vec{\mu}_{s_2^k} \,.\, \beta_{s_2^k}(\vec{\nu}_{s_2^k})\, \nabla_s\, \varkappa_{\gamma,s_2^k} = o_3^k\, \vec{\mu}_{s_3^k} \,.\, \beta_{s_3^k}(\vec{\nu}_{s_3^k})\, \nabla_s\, \varkappa_{\gamma,s_3^k} \quad \text{on } \mathcal{T}_k\,, \quad k = 1 \to I_T, \tag{1.21b}$$

$$\sum_{j=1}^{3} o_j^k\, \varkappa_{\gamma,s_j^k} = 0 \quad \text{on } \mathcal{T}_k\,, \quad k = 1 \to I_T\,. \tag{1.21c}$$

We note that in the isotropic case, (1.14), it holds that $\vec{\nu}_{\gamma,i} = \sigma_i\, \vec{\nu}_i$ with $\varkappa_{\gamma,i} = \sigma_i\, \varkappa_i$, and hence (1.21a–c) with $\beta = (1, \ldots, 1)$, on recalling that $\vec{\nu}_i \,.\, \vec{\mu}_i = 0$, simplify to $\sum_{j=1}^3 \sigma_{s_j^k}\, \vec{\mu}_{s_j^k} = \vec{0}$, $o_1^k\, \sigma_{s_1^k}\, \vec{\mu}_{s_1^k} \,.\, \nabla_s\, \varkappa_{s_1^k} = o_2^k\, \sigma_{s_2^k}\, \vec{\mu}_{s_2^k} \,.\, \nabla_s\, \varkappa_{s_2^k} = o_3^k\, \sigma_{s_3^k}\, \vec{\mu}_{s_3^k} \,.\, \nabla_s\, \varkappa_{s_3^k}$ and $\sum_{j=1}^3 o_j^k\, \sigma_{s_j^k}\, \varkappa_{s_j^k} = 0$ on $\mathcal{T}_k$ for $k = 1 \to I_T$; respectively. Hence we observe that (1.21a–c) collapse to (1.4b–d) in the isotropic equal energy density case.

As in the isotropic case, (1.10a,b) and (1.11a,b), we are able to obtain the following weak formulations, see Section 2 for details. For anisotropic mean curvature flow we obtain: Find $\vec{x} \in \underline{V}(\Omega)$ and $\varkappa_\gamma \in \widehat{W}(\Gamma)$ such that

$$\langle \vec{x}_t, \eta\, \vec{\nu} \rangle - \langle \beta(\vec{\nu})\, \varkappa_\gamma, \eta \rangle = 0 \qquad \forall\ \eta \in \widehat{W}(\Gamma)\,, \tag{1.22a}$$

$$\langle \varkappa_\gamma\, \vec{\nu}, \vec{\chi} \rangle + \langle \nabla_s^{\widetilde{G}}\, \vec{x}, \nabla_s^{\widetilde{G}}\, \vec{\chi} \rangle_\gamma = 0 \qquad \forall\ \vec{\chi} \in \underline{V}(\Gamma)\,. \tag{1.22b}$$

For anisotropic surface diffusion flow we obtain: Find $\vec{x} \in \underline{V}(\Omega)$ and $\varkappa_\gamma \in W(\Gamma)$ such that

$$\langle \vec{x}_t, \eta\, \vec{\nu} \rangle - \langle \beta(\vec{\nu})\, \nabla_s\, \varkappa_\gamma, \nabla_s\, \eta \rangle = 0 \qquad \forall\ \eta \in W(\Gamma)\,, \tag{1.23a}$$

$$\langle \varkappa_\gamma\, \vec{\nu}, \vec{\chi} \rangle + \langle \nabla_s^{\widetilde{G}}\, \vec{x}, \nabla_s^{\widetilde{G}}\, \vec{\chi} \rangle_\gamma = 0 \qquad \forall\ \vec{\chi} \in \underline{V}(\Gamma)\,. \tag{1.23b}$$

Here we have introduced the shorthand notation $\langle \nabla_s^{\widetilde{G}} \cdot, \nabla_s^{\widetilde{G}} \cdot \rangle_\gamma$ for the natural cluster analogue of the inner product defined in Barrett, Garcke, and Nürnberg (2008c). This is defined as follows. First, we introduce the symmetric positive definite matrices $\widetilde{G}_i^{(\ell)}$ with the associated inner products $(\cdot, \cdot)_{\widetilde{G}_i^{(\ell)}}$ on $\mathbb{R}^3$ by

$$\widetilde{G}_i^{(\ell)} := [\det G_i^{(\ell)}]^{\frac{1}{2}}\, [G_i^{(\ell)}]^{-1} \qquad \text{and} \qquad (\vec{a}, \vec{b})_{\widetilde{G}_i^{(\ell)}} = \vec{a} \,.\, \widetilde{G}_i^{(\ell)}\, \vec{b} \qquad \forall\ \vec{a},\, \vec{b} \in \mathbb{R}^3\,, \quad \ell = 1 \to L_i, \qquad i = 1 \to I_S\,.$$

With $\{\vec{p}, \vec{\tau}_1, \vec{\tau}_2\}$ an orthonormal basis for $\mathbb{R}^3$, it follows, on recalling (1.15), that

$$\gamma_i^{(\ell)}(\vec{p}) = [\det B_i^{(\ell)}]^{\frac{1}{2}}, \quad \text{where } B_i^{(\ell)} \in \mathbb{R}^2 \ \text{ with } \ [B_i^{(\ell)}]_{jk} = (\vec{\tau}_j, \vec{\tau}_k)_{\widetilde{G}_i^{(\ell)}}\,, \quad j, k = 1 \to 2\,;$$

see Barrett, Garcke, and Nürnberg (2008c, Lemma 2.1). Secondly, we set

$$H_i^{(\ell)} := [D\vec{x}_i]^T\, \widetilde{G}_i^{(\ell)}\, D\vec{x}_i \qquad \text{and} \qquad [h_i^{(\ell)}]^{jk} := [(H_i^{(\ell)})^{-1}]_{jk}\,, \quad j, k = 1 \to 2\,,$$

where $D\vec{x}_i$ denotes the Jacobian matrix. Then we have that

$$\langle \nabla_s^{\widetilde{G}}\,\vec{\eta}, \nabla_s^{\widetilde{G}}\,\vec{\chi}\rangle_\gamma := \sum_{i=1}^{I_S}\sum_{\ell=1}^{L_i}\int_{\Gamma_i}\left[\frac{\gamma_i^{(\ell)}(\vec{\nu}_i)}{\gamma_i(\vec{\nu}_i)}\right]^{r_i-1}(\nabla_s^{\widetilde{G}_i^{(\ell)}}\,\vec{\eta}_i, \nabla_s^{\widetilde{G}_i^{(\ell)}}\,\vec{\chi}_i)_{\widetilde{G}_i^{(\ell)}}\,\gamma_i^{(\ell)}(\vec{\nu}_i)\,\mathrm{d}\mathcal{H}^2\,, \tag{1.24a}$$

where for all smooth $\vec{\eta}_i,\ \vec{\chi}_i : \Gamma_i \to \mathbb{R}^3$

$$\begin{aligned}(\nabla_s^{\widetilde{G}_i^{(\ell)}}\,\vec{\eta}_i, \nabla_s^{\widetilde{G}_i^{(\ell)}}\,\vec{\chi}_i)_{\widetilde{G}_i^{(\ell)}} &:= \sum_{j=1}^{2}(\partial_{\vec{t}_{i,j}^{(\ell)}}\,\vec{\eta}_i, \partial_{\vec{t}_{i,j}^{(\ell)}}\,\vec{\chi}_i)_{\widetilde{G}_i^{(\ell)}}\\ &= \sum_{j=1}^{2}\sum_{k=1}^{2}[h_i^{(\ell)}]^{jk}\,(\partial_k[\vec{\eta}_i\circ\vec{x}_i], \partial_j[\vec{\chi}_i\circ\vec{x}_i])_{\widetilde{G}_i^{(\ell)}}\end{aligned} \tag{1.24b}$$

with $\{\vec{t}_{i,1}^{(\ell)}, \vec{t}_{i,2}^{(\ell)}\}$ being an orthonormal basis with respect to the $\widetilde{G}_i^{(\ell)}$ inner product for the tangent plane of Γ_i; see Barrett, Garcke, and Nürnberg (2008c, (2.8), (2.11), (2.20)) for further details.

We remark that for equal isotropic energies $\gamma_i(\cdot) = |\cdot|$, $i = 1 \to I_S$, the formulations (1.22a,b) and (1.23a,b) collapse to their isotropic counterparts (1.10a,b) and (1.11a,b), respectively. We recall that the novel variational formulation in Barrett, Garcke, and Nürnberg (2008c) has yielded the first unconditionally stable parametric approximations of anisotropic geometric evolution equations in higher dimensions. Recently, an alternative stable finite element approximation for anisotropic mean curvature flow for closed hypersurfaces in $\mathbb{R}^3$ has been introduced in Pozzi (2008). For convex anisotropies, on employing a stabilizing term that slightly changes the approximated flow, stability was shown for a fully discrete approximation. However, we stress that this approximation cannot be generalized to the case of surface clusters considered in this paper.

Finally, we will also consider situations in which parts of the boundaries of the surfaces Γ_i, $i = 1 \to I_S$, are constrained to lie on the boundary $\partial\mathcal{D}$ of a domain $\mathcal{D}$. In this case, boundary conditions have to hold on these I_B, $I_B \geq 0$, boundary lines. We introduce the following notation to formulate the necessary conditions. Let the boundary line $\mathcal{B}_k$ be given by the pair (s_k, p_k) such that, similarly to (1.4a),

$$\mathcal{B}_k(t) := \vec{x}_{s_k}(\partial_{p_k}\Omega_{s_k}, t) \subset \partial\mathcal{D}, \qquad k = 1 \to I_B\,. \tag{1.25}$$

We note that throughout this paper, we assume for simplicity that

$$\bigcup_{k=1}^{I_B}\{(s_k,p_k)\} \cap \bigcup_{k=1}^{I_T}\bigcup_{j=1}^{3}\{(s_j^k, p_j^k)\} = \emptyset\,,$$

i.e. that no triple junction line $\mathcal{T}_k$ is constrained to lie on the boundary $\partial\mathcal{D}$. This still leaves the possibility open that a triple junction line meets the boundary $\partial\mathcal{D}$ at e.g. a single point. In such a case, no extra conditions are needed at these points. In addition, we assume that

$$(i,p) \in \bigcup_{k=1}^{I_B}\{(s_k,p_k)\} \cup \bigcup_{k=1}^{I_T}\bigcup_{j=1}^{3}\{(s_j^k, p_j^k)\}\,, \qquad p = 1 \to I_P^i, \quad i = 1 \to I_S\,;$$

i.e. that each part of the partitioned boundaries $\partial\Omega_i$ is mapped by $\vec{x}$ either to a triple junction line, or to a boundary line. Let $\vec{n}$ be the outer unit normal to $\partial\mathcal{D}$. Then (1.25) can be equivalently formulated as $\vec{x}_{s_k}(\partial_{p_k}\Omega_{s_k}) \subset \partial\mathcal{D}$ at time $t = 0$ together with

$$\vec{n} \,.\, \vec{x}_{s_k,t} = 0 \quad \text{on } \mathcal{B}_k\,, \qquad k = 1 \to I_B\,. \tag{1.26a}$$

In the case of anisotropic curvature flow we require in addition that

$$\vec{n} \,.\, \gamma'_{s_k}(\vec{\nu}_{s_k}) = 0 \quad \text{on } \mathcal{B}_k\,, \qquad k = 1 \to I_B\,, \tag{1.26b}$$

which collapses to a 90° angle condition, $\vec{n} \,.\, \vec{\nu}_{s_k} = 0$, in the case of isotropic γ_{s_k}. In the case of anisotropic surface diffusion we require, in addition to (1.26b), the no-flux boundary condition

$$\vec{\mu}_{s_k} \,.\, \nabla_s \varkappa_{\gamma,s_k} = 0 \quad \text{on } \mathcal{B}_k\,, \qquad k = 1 \to I_B\,. \tag{1.26c}$$

This condition has been introduced for curves in the plane by Garcke and Novick-Cohen (2000) in the isotropic case, and was generalized by Barrett, Garcke, and Nürnberg (2008a) to the anisotropic case. The condition (1.26c) is the natural generalization of these conditions in the plane to the case of surfaces in $\mathbb{R}^3$.

2 Derivation of the governing equations

In this section, we will derive the governing equations for anisotropic mean curvature flow, i.e. the weighted L^2-gradient flow of (1.12), and anisotropic surface diffusion, i.e. the weighted H^{-1}-gradient flow of (1.12), for surface clusters in $\mathbb{R}^3$. We will only consider the general anisotropic situation, and so the isotropic case will just be a specific example of this. First we state a transport theorem for anisotropic energies.

LEMMA. 2.1. *Let $\vec{x}_i : \overline{\Omega}_i \times (-\delta_0, \delta_0) \to \mathbb{R}^3$ be a smooth parameterization of an evolving hypersurface $(\Gamma_i^\delta)_{|\delta|<\delta_0}$ in $\mathbb{R}^3$, where $\Omega_i \subset \mathbb{R}^2$ is a smooth domain. Let $\vec{\nu}_i^\delta$ be a unit normal field to Γ_i^δ, and let $\vec{\mu}_i^\delta$ be the conormal to $\partial\Gamma_i^\delta$. In addition, let $\gamma_i : \mathbb{R}^3 \to \mathbb{R}_{\geq 0}$ be a given anisotropy function satisfying* (1.13). *Then it holds that*

$$\frac{\mathrm{d}}{\mathrm{d}\delta} \int_{\Gamma_i^\delta} \gamma_i(\vec{\nu}_i^\delta)\, \mathrm{d}\mathcal{H}^2 = \int_{\Gamma_i^\delta} \mathcal{V}_i^\delta \, \nabla_s \,.\, \gamma_i'(\vec{\nu}_i^\delta)\, \mathrm{d}\mathcal{H}^2 + \int_{\partial\Gamma_i^\delta} \vec{x}_{i,\delta} \,.\, (\gamma_i(\vec{\nu}_i^\delta)\, \vec{\mu}_i^\delta - (\gamma_i'(\vec{\nu}_i^\delta) \,.\, \vec{\mu}_i^\delta)\, \vec{\nu}_i^\delta)\, \mathrm{d}\mathcal{H}^1,$$

where $\vec{x}_{i,\delta} := \frac{\mathrm{d}}{\mathrm{d}\delta}\, \vec{x}_i$ and $\mathcal{V}_i^\delta := \vec{x}_{i,\delta} \,.\, \vec{\nu}_i^\delta$ is the normal velocity of Γ_i^δ.

Proof. Using a transport theorem, which can be found for example in Gurtin (2000, (15-31)) and Garcke and Wieland (2006, (2.9)), we obtain that

$$\frac{\mathrm{d}}{\mathrm{d}\delta} \int_{\Gamma_i^\delta} \gamma_i(\vec{\nu}_i^\delta)\, \mathrm{d}\mathcal{H}^2 = \int_{\Gamma_i^\delta} (\partial^0\, \gamma_i(\vec{\nu}_i^\delta) - \gamma_i(\vec{\nu}_i^\delta)\, \mathcal{V}_i^\delta\, \varkappa_i^\delta)\, \mathrm{d}\mathcal{H}^2 + \int_{\partial\Gamma_i^\delta} \gamma_i(\vec{\nu}_i^\delta)\, \vec{x}_{i,\delta} \,.\, \vec{\mu}_i^\delta\, \mathrm{d}\mathcal{H}^1\,,$$

where ∂^0 is the time derivative following Γ_i^δ, see Gurtin (2000, (15-21)) and $\varkappa_i^\delta$ is the sum of principal curvatures of Γ_i^δ. Since $\partial^0\, \vec{\nu}_i^\delta = -\nabla_s\, \mathcal{V}_i^\delta$, see Gurtin (2000, (15-24)), we obtain

the desired result by using integration by parts on manifolds, see e.g. Betounes (1986, Corollary 4), and the identity $\gamma_i'(\vec{p}) \,.\, \vec{p} = \gamma_i(\vec{p})$. ☐

Applying the above lemma locally in a situation where the three surfaces $\Gamma_{s_1^k}, \Gamma_{s_2^k}, \Gamma_{s_3^k}$, with surface energy densities $\gamma_{s_1^k}, \gamma_{s_2^k}, \gamma_{s_3^k}$, meet at a triple junction line $\mathcal{T}_k$, we obtain the condition

$$\sum_{j=1}^{3} \left[\gamma_{s_j^k}(\vec{\nu}_{s_j^k})\, \vec{\mu}_{s_j^k} - (\gamma_{s_j^k}'(\vec{\nu}_{s_j^k}) \,.\, \vec{\mu}_{s_j^k})\, \vec{\nu}_{s_j^k} \right] = \vec{0} \quad \text{on } \mathcal{T}_k \,, \tag{2.1}$$

i.e. (1.21a), in order for this boundary term on $\mathcal{T}_k$ to vanish. We remark that the vectors $\vec{\nu}_{s_j^k}, \vec{\mu}_{s_j^k}$, $j = 1 \to 3$, all lie in the plane T_k perpendicular to the triple junction line $\mathcal{T}_k$; see Figure 1. We recall also the choice of (o_1^k, o_2^k, o_3^k) so that $(o_j^k\, \vec{\nu}_{s_j^k}, \vec{\mu}_{s_j^k})$, $j = 1 \to 3$, have the same orientation. Noting that $\gamma_i'(\vec{p}_i) \,.\, \vec{p} = \gamma_i(\vec{p}) = \gamma_i(-\vec{p}) = -\gamma_i'(-\vec{p}_i) \,.\, \vec{p}$, it follows from (2.1) that

$$\sum_{j=1}^{3} \left[(\gamma_{s_j^k}'(o_j^k\, \vec{\nu}_{s_j^k}) \,.\, (o_j^k\, \vec{\nu}_{s_j^k}))\, \vec{\mu}_{s_j^k} - (\gamma_{s_j^k}'(o_j^k\, \vec{\nu}_{s_j^k}) \,.\, \vec{\mu}_{s_j^k})\, (o_j^k\, \vec{\nu}_{s_j^k}) \right] = \vec{0} \quad \text{on } \mathcal{T}_k \,. \tag{2.2}$$

Hence on rotating the left-hand side of (2.2) by 90° in the plane T_k, we deduce that (2.2) is equivalent to

$$\sum_{j=1}^{3} \Pi_{|T_k} \gamma_{s_j^k}'(o_j^k\, \vec{\nu}_{s_j^k}) = \vec{0} \quad \text{on } \mathcal{T}_k \,, \tag{2.3}$$

where $\Pi_{|T_k}$ is the orthogonal projection onto the plane T_k. The identity (2.1) can be interpreted as a force balance on the triple junction line $\mathcal{T}_k$, see Cahn and Hoffmann (1974) and Garcke and Nestler (2000). It simplifies in the isotropic case, (1.14), to $\sum_{j=1}^{3} \sigma_{s_j^k}\, \vec{\nu}_{s_j^k} = \vec{0}$, which for equal isotropic surface energies is equivalent to (1.4b).

If we require that parts of the boundaries of Γ remain on $\partial\mathcal{D}$, we need to deduce additional conditions. With $\vec{n}$ the outer unit normal to $\partial\mathcal{D}$, we first of all require that $\vec{n} \,.\, \vec{x}_{s_k,t} = 0$ on $\mathcal{B}_k \subset \partial\Gamma_{s_k} \cap \partial\mathcal{D}$, i.e. (1.26a), in order to obtain that this part of $\partial\Gamma_{s_k}$ remains on $\partial\mathcal{D}$, for $k = 1 \to I_B$. In addition, for $k = 1 \to I_B$, we require that

$$\vec{x}_{s_k,t} \,.\, (\gamma_{s_k}(\vec{\nu}_{s_k})\, \vec{\mu}_{s_k} - (\gamma_{s_k}'(\vec{\nu}_{s_k}) \,.\, \vec{\mu}_{s_k})\, \vec{\nu}_{s_k}) = 0 \quad \text{on } \mathcal{B}_k \tag{2.4}$$

for all $\vec{n} \,.\, \vec{x}_{s_k,t} = 0$ on $\mathcal{B}_k$ in order for this boundary term to vanish. We note that $\vec{\nu}_{s_k}$, $\vec{\mu}_{s_k}$, $\vec{n}$ all lie in the plane B_k perpendicular to $\mathcal{B}_k$. In addition, we note that (2.4) is equivalent to the vector $\gamma_{s_k}(\vec{\nu}_{s_k})\, \vec{\mu}_{s_k} - (\gamma_{s_k}'(\vec{\nu}_{s_k}) \,.\, \vec{\mu}_{s_k})\, \vec{\nu}_{s_k}$ being a multiple of $\vec{n}$, and so a 90° degree rotation in the plane B_k of this vector yields, similarly to (2.3), that

$$\vec{n} \,.\, (\Pi_{|B_k}\, \gamma_{s_k}'(\vec{\nu}_{s_k})) = 0 \quad \text{on } \mathcal{B}_k \,,$$

where $\Pi_{|B_k}$ is the orthogonal projection onto the plane B_k. Since $\vec{n} \in B_k$, we obtain that the I_B boundary conditions (2.4) are equivalent to (1.26a,b).

Using Lemma 2.1 and recalling (1.18a,b), we now deduce that surface clusters, with triple junctions lines, evolving by the anisotropic mean curvature law (1.19) together with

the attachment conditions (1.4a) and the boundary conditions (1.21a) fulfill the energy inequality

$$\frac{\mathrm{d}}{\mathrm{d}t}\,E_\gamma(\Gamma) = \frac{\mathrm{d}}{\mathrm{d}t}\left(\sum_{i=1}^{I_S}\int_{\Gamma_i}\gamma_i(\vec\nu_i)\,\mathrm{d}\mathcal{H}^2\right) = -\sum_{i=1}^{I_S}\int_{\Gamma_i}\frac{1}{\beta_i(\vec\nu_i)}\,\mathcal{V}_i^2\,\mathrm{d}\mathcal{H}^2 \le 0\,. \tag{2.5}$$

This proves that (1.19) with (1.4a), (1.21a) is the (weighted) L^2-gradient flow of $E_\gamma(\Gamma)$. In addition, it is easily seen that (2.5) remains valid if parts of $\partial\Gamma_i$ are constrained to lie on $\partial\mathcal{D}$, i.e. if the boundary conditions (1.26a,b) are imposed.

Similarly, in the case of surface clusters, with triple junctions lines, evolving by the anisotropic surface diffusion law (1.20), together with the attachment conditions (1.4a) and the boundary conditions (1.21a–c), we deduce that

$$\begin{aligned}\frac{\mathrm{d}}{\mathrm{d}t}\,E_\gamma(\Gamma) &= \sum_{i=1}^{I_S}\int_{\Gamma_i}\mathcal{V}_i\,\nabla_s\,.\,(\gamma'(\vec\nu_i))\,\mathrm{d}\mathcal{H}^2 = \sum_{i=1}^{I_S}\int_{\Gamma_i}\nabla_s\,.\,(\beta_i(\vec\nu_i)\,\nabla_s\,\varkappa_{\gamma,i})\,\varkappa_{\gamma,i}\,\mathrm{d}\mathcal{H}^2\\ &= -\sum_{i=1}^{I_S}\int_{\Gamma_i}\beta_i(\vec\nu_i)\,|\nabla_s\,\varkappa_{\gamma,i}|^2\,\mathrm{d}\mathcal{H}^2 \le 0\,,\end{aligned} \tag{2.6}$$

where the boundary terms which arise from performing integration by parts vanish as (1.21b,c) imply that for $k = 1 \to I_T$

$$\sum_{j=1}^{3}\varkappa_{\gamma,s_j^k}\,\beta_{s_j^k}(\vec\nu_{s_j^k})\nabla_s\,\varkappa_{\gamma,s_j^k}\,.\,\vec\mu_{s_j^k} = 0 \quad \text{on } \mathcal{T}_k\,. \tag{2.7}$$

On noting that $\varkappa_{\gamma,i}$ is minus the inverse of the weighted surface Laplacian defined in (1.20) acting on $\mathcal{V}_i$, we see from (2.6) that (1.20) with (1.4a), (1.21a–c) is the (weighted) H^{-1}-gradient flow of $E_\gamma(\Gamma)$. Once again, it is easily seen that (2.6) remains valid if parts of $\partial\Gamma_i$ are constrained to lie on $\partial\mathcal{D}$ if the boundary conditions (1.26a–c) are imposed.

In the remainder of this section, we restrict ourselves to the class of anisotropies (1.15) and derive the weak formulations (1.22a,b) and (1.23a,b). First we compute the first variation of the anisotropic surface energy (1.12).

LEMMA. 2.2. *Let E_γ be given by* (1.12) *with $\gamma = (\gamma_1, \ldots, \gamma_{I_S})$ as in* (1.15). *Furthermore let $\vec g \in \underline{V}(\Gamma)$ be a smooth vector field and*

$$\Gamma^\delta := \{\vec z + \delta\,\vec g(\vec z) : \vec z \in \Gamma = \vec x(\Omega)\}\,. \tag{2.8}$$

Then, on recalling (1.24a,b), *we obtain that*

$$\frac{\mathrm{d}}{\mathrm{d}\delta}\,E_\gamma(\Gamma^\delta)\,|_{\delta=0} = \langle\nabla_s^{\widetilde G}\,\vec x, \nabla_s^{\widetilde G}\,\vec g\rangle_\gamma\,. \tag{2.9}$$

Proof. We use the same arguments as in the proofs of Barrett, Garcke, and Nürnberg (2008c, Lemma 2.5,Theorem 2.1) to compute the first variation of $\int_{\Gamma_i}\gamma_i(\vec\nu_i)\,\mathrm{d}\mathcal{H}^2$. We

note that the arguments applied there to closed surfaces remain true for surfaces Γ_i, $i = 1 \to I_S$, with boundaries $\partial\Gamma_i$. We briefly outline the key steps of the proof.

First, we consider the case of Γ_i, where γ_i is defined by (1.15) with $L_i = 1$. Then combining Barrett, Garcke, and Nürnberg (2008c, Lemma 2.5, Lemma 2.2, (2.19b)) with (1.24b) yields that

$$\begin{aligned}\frac{\mathrm{d}}{\mathrm{d}\delta}\int_{\Gamma_i}\gamma_i(\vec{\nu}_i)\,\mathrm{d}\mathcal{H}^2\,|_{\delta=0} &= \int_{\Omega_i}\sum_{j=1}^{2}\sum_{k=1}^{2}[h_i^{(1)}]^{jk}\,(\partial_k\vec{x}_i,\partial_j[\vec{g}_i\circ\vec{x}_i])_{\widetilde{G}_i^{(1)}}\,[\det H_i^{(1)}]^{\frac{1}{2}}\,\mathrm{d}\mathcal{L}^2\\ &= \int_{\Gamma_i}(\nabla_s^{\widetilde{G}_i^{(1)}}\,\vec{x}_i,\nabla_s^{\widetilde{G}_i^{(1)}}\,\vec{g}_i)_{\widetilde{G}_i^{(1)}}\,\gamma_i(\vec{\nu}_i)\,\mathrm{d}\mathcal{H}^2\,, \end{aligned}\tag{2.10}$$

where $\mathcal{L}^d$ denotes the Lebesgue measure in $\mathbb{R}^d$.

The extension of (2.10) to $L_i \geq 1$ and $r_i \in [1,\infty)$ follows from combining Barrett, Garcke, and Nürnberg (2008c, (2.45), Lemma 2.2, (2.19b)) and (1.24b), and we obtain that

$$\frac{\mathrm{d}}{\mathrm{d}\delta}\int_{\Gamma_i}\gamma_i(\vec{\nu}_i)\,\mathrm{d}\mathcal{H}^2\,|_{\delta=0} = \sum_{\ell=1}^{L_i}\int_{\Gamma_i}\left[\frac{\gamma_i^{(\ell)}(\vec{\nu}_i)}{\gamma_i(\vec{\nu}_i)}\right]^{r_i-1}(\nabla_s^{\widetilde{G}_i^{(\ell)}}\,\vec{x}_i,\nabla_s^{\widetilde{G}_i^{(\ell)}}\,\vec{g}_i)_{\widetilde{G}_i^{(\ell)}}\,\gamma_i^{(\ell)}(\vec{\nu}_i)\,\mathrm{d}\mathcal{H}^2\,.\tag{2.11}$$

Summing (2.11) for $i = 1 \to I_S$ then yields the desired result (2.9), on recalling the definitions (1.12) and (1.24a). ∎

LEMMA. 2.3. *Let γ be given by* (1.15). *Then for smooth Γ we obtain that its parameterization $\vec{x} \in \underline{V}(\Omega)$ satisfying*

$$\langle\varkappa_\gamma\,\vec{\nu},\vec{\chi}\rangle + \langle\nabla_s^{\widetilde{G}}\,\vec{x},\nabla_s^{\widetilde{G}}\,\vec{\chi}\rangle_\gamma = 0 \qquad \forall\ \vec{\chi} \in \underline{V}(\Gamma)$$

is equivalent to (1.18a,b) *together with the attachment conditions* (1.4a) *and the boundary conditions* (1.21a).

Proof. Combining the results in Lemmas 2.1 and 2.2 for the evolving hypersurfaces Γ^δ in (2.8) we obtain, as $\vec{x}_{i,\delta} = \vec{g}$, that

$$\langle\nabla_s^{\widetilde{G}}\,\vec{x},\nabla_s^{\widetilde{G}}\,\vec{g}\rangle_\gamma = \sum_{i=1}^{I_S}\int_{\Gamma_i}(\vec{g}\,.\,\vec{\nu}_i)\,\nabla_s\,.\,\gamma_i'(\vec{\nu}_i)\,\mathrm{d}\mathcal{H}^2 + \sum_{i=1}^{I_S}\int_{\partial\Gamma_i}\vec{g}\,.\,(\gamma_i(\vec{\nu}_i)\,\vec{\mu}_i - (\gamma_i'(\vec{\nu}_i)\,.\,\vec{\mu}_i)\,\vec{\nu}_i)\,\mathrm{d}\mathcal{H}^1\,.$$

Since the above identity has to hold for all $\vec{g} \in \underline{V}(\Gamma)$, we obtain, for $k = 1 \to I_T$, that the integrals on the triple junction lines $\mathcal{T}_k$ have to vanish, and hence the boundary conditions (1.21a) have to hold. Then taking (1.18a,b) into account we have that

$$\langle\varkappa_\gamma\,\vec{\nu},\vec{g}\rangle = -\langle(\nabla_s\,.\,\gamma'(\vec{\nu}))\,\vec{\nu},\vec{g}\rangle \qquad \forall\ \vec{g} \in \underline{V}(\Gamma)\,,$$

and hence the desired equivalence follows. ∎

Let

$$\underline{V}_\partial(\Gamma) := \{\vec{\chi} \in \underline{V}(\Gamma) : \vec{n}\,.\,\vec{\chi}_{s_k} = 0 \quad \text{on} \quad \mathcal{B}_k, \quad k = 1 \to I_B\}\,.\tag{2.12}$$

COROLLARY. 2.1. *Let the assumptions of Lemma 2.2 hold. In addition, let* $\vec{g} \in \underline{V}_\partial(\Gamma)$ *and let* Γ^δ *be defined by* (2.8)*. Then we obtain that*

$$\frac{\mathrm{d}}{\mathrm{d}\delta} E_\gamma(\Gamma^\delta) \mid_{\delta=0} = \langle \nabla_s^{\widetilde{G}} \vec{x}, \nabla_s^{\widetilde{G}} \vec{g} \rangle_\gamma \,. \tag{2.13}$$

Moreover, for smooth Γ *with boundary intersections we obtain that its parameterization* $\vec{x} \in \underline{V}(\Omega)$ *satisfying* (1.26a) *and*

$$\langle \varkappa_\gamma \, \vec{\nu}, \vec{\chi} \rangle + \langle \nabla_s^{\widetilde{G}} \vec{x}, \nabla_s^{\widetilde{G}} \vec{\chi} \rangle_\gamma = 0 \qquad \forall \ \vec{\chi} \in \underline{V}_\partial(\Gamma) \tag{2.14}$$

is equivalent to (1.18a,b)*, the attachment conditions* (1.4a) *and the triple junction line conditions* (1.21a)*, together with the boundary line conditions* (1.26a,b)*.*

Proof. The proof of (2.13) is exactly the same as the one for (2.9), except that the variation is over $\vec{g} \in \underline{V}_\partial(\Gamma)$ as opposed to $\vec{g} \in \underline{V}(\Gamma)$. The equivalence statement follows as in the proof of Lemma 2.3 on recalling the equivalence of the boundary conditions (2.4), $k = 1 \to I_B$, and (1.26a,b). ☐

THEOREM. 2.1. *Let* γ *be given by* (1.15)*. Then for a smooth family of evolving surface clusters* $(\Gamma(t))_{t \geq 0}$ *the weak formulations* (1.22a,b) *and* (1.23a,b) *are equivalent to the strong formulations* (1.19) *with* (1.4a), (1.21a) *and* (1.20) *with* (1.4a), (1.21a–c)*, respectively. Similarly,* (2.14) *together with* (1.22a) *or* (1.23a) *is a weak formulation of the corresponding flows when the boundary line conditions* (1.26b) *and* (1.26b,c) *are present, respectively.*

Proof. The proof for (1.22a,b) follows immediately from Lemma 2.3 and multiplying (1.19) with a test function $\eta \in \widehat{W}(\Gamma)$. Similarly, the proof for (1.23a,b) follows from Lemma 2.3, multiplying (1.20) with a test function $\eta \in W(\Gamma)$ and doing integration by parts on noting (1.21b) and (1.6b), similarly to (2.6); recall (2.7). The final statement follows from Corollary 2.1 and the above. ☐

REMARK. 2.1. *Based on* (1.23a,b)*, it is now straightforward to show that anisotropic surface diffusion preserves the enclosed volumes. We illustrate this with an example. Consider a double bubble cluster as shown in Figure 4, with* $(o_1^1, o_2^1, o_3^1) = (1, 1, 1)$ *and* $\vec{\nu}_1$ *chosen as the outer normal to the volume enclosed by* Γ_1 *and* Γ_2*, which implies that* $\vec{\nu}_2$ *is the inner normal to this volume, which we denote by* v*. Then choosing* $\chi = (1, -1, 0) \in W(\Gamma)$ *in* (1.23a) *yields that*

$$\frac{\mathrm{d}}{\mathrm{d}t} \mathcal{L}^3(v) = \int_{\Gamma_1} [\vec{x}_1]_t \,.\, \vec{\nu}_1 \, \mathrm{d}\mathcal{H}^2 - \int_{\Gamma_2} [\vec{x}_2]_t \,.\, \vec{\nu}_2 \, \mathrm{d}\mathcal{H}^2 = 0 \,,$$

i.e. the volume of v *is preserved.*

3 Parametric finite element approximation

For $i \to I_S$, let Ω_i^h be a triangulation approximating $\overline{\Omega}_i \subset \mathbb{R}^2$, so that $\Omega_i^h = \cup_{j=1}^{J_i} \overline{\sigma_j^i}$, where $\{\sigma_j^i\}_{j=1}^{J_i}$ is a family of mutually disjoint open triangles with vertices $\{\vec{q}_k^{\,i}\}_{k=1}^{K_i}$. In

particular, let $\{\vec{q}_k^{\,i}\}_{k=1}^{\overline{K}_i}$ denote the vertices in the interior of Ω_i^h and let $\{\vec{q}_k^{\,i}\}_{k=\overline{K}_i+1}^{K_i}$ denote the vertices on $\partial\Omega_i^h$. We set $h := \max_{i=1\to I_S} \max_{j=1\to J_i} \operatorname{diam}(\sigma_j^i)$. We introduce the finite element space $\underline{\widehat{V}}^h(\Omega^h) := \{\vec{\chi} \in \overset{I_S}{\underset{i=1}{\times}} C(\Omega_i^h, \mathbb{R}^3) : \vec{\chi}_i|_{\sigma_j^i} \text{ is linear } \forall\ j = 1 \to J_i,\ i = 1 \to I_S\}$. In order to describe the conditions that our discretization needs to satisfy at the triple junction lines, we have to make the following compatibility assumptions. Let $\partial_j\Omega_i^h$ be the polygonal curve approximating $\partial_j\Omega_i$, $j = 1 \to I_P^i$, $i = 1 \to I_S$. Then we assume that the endpoints of $\partial_j\Omega_i^h$ and $\partial_j\Omega_i$ coincide and that

$$Z_k := \#\{\{\vec{q}_l^{\,s_1^k}\}_{l=1}^{K_{s_1^k}} \cap \partial_{p_1^k}\Omega^h_{s_1^k}\} = \#\{\{\vec{q}_l^{\,s_2^k}\}_{l=1}^{K_{s_2^k}} \cap \partial_{p_2^k}\Omega^h_{s_2^k}\} = \#\{\{\vec{q}_l^{\,s_3^k}\}_{l=1}^{K_{s_3^k}} \cap \partial_{p_3^k}\Omega^h_{s_3^k}\} \tag{3.1}$$

for all $k = 1 \to I_T$. The condition (3.1) simply says that the triangulations of Ω^h need to "match up" at their boundaries, where they meet at triple junction lines. In addition, let

$$\vec{\rho}_j^{\,k} : \{1 \to Z_k\} \to \{\{\vec{q}_l^{\,s_j^k}\}_{l=1}^{K_{s_j^k}} \cap \partial_{p_j^k}\Omega^h_{s_j^k}\}\,, \qquad j = 1 \to 3\,, \tag{3.2}$$

be a bijective map such that $(\vec{\rho}_j^{\,k}(1), \ldots, \vec{\rho}_j^{\,k}(Z_k))$ is an ordered sequence of vertices of the polygonal curve $\partial_{p_j^k}\Omega^h_{s_j^k}$, $j = 1 \to 3$, $k = 1 \to I_T$.

Then we define the natural discrete analogue of $\underline{V}(\Omega)$ by $\underline{V}^h(\Omega^h) := \{\vec{\chi} \in \underline{\widehat{V}}^h(\Omega^h) : \vec{\chi}_{s_1^k}(\vec{\rho}_1^{\,k}(l)) = \vec{\chi}_{s_2^k}(\vec{\rho}_2^{\,k}(l)) = \vec{\chi}_{s_3^k}(\vec{\rho}_3^{\,k}(l))\,,\ l = 1 \to Z_k,\ k = 1 \to I_T\}$.

Let $0 = t_0 < t_1 < \ldots < t_{M-1} < t_M = T$ be a partitioning of $[0, T]$ into possibly variable time steps $\tau_m := t_{m+1} - t_m$, $m = 0 \to M-1$.

The surfaces Γ_i^m are now given by their parameterizations $\vec{X}_i^m$, $i = 1 \to I_S$, where $\vec{X}^m \in \underline{\widehat{V}}^h(\Omega^h)$. We set $\Gamma^m := \vec{X}^m(\Omega^h)$ and observe that, with the above definitions, the polygonal curves $\mathcal{T}_k^m$ defined by the ordered sequence of vertices $(\vec{X}^m_{s_1^k}(\vec{\rho}_1^{\,k}(1)), \ldots, \vec{X}^m_{s_1^k}(\vec{\rho}_1^{\,k}(Z_k)))$, $k = 1 \to I_T$, are the triple junction lines of the polyhedral surface cluster Γ^m. These will now be used to defined the necessary finite element spaces on Γ^m. Let $\sigma_j^{m,i} := \vec{X}_i^m(\sigma_j^i)$ and similarly $\vec{q}_k^{\,m,i} := \vec{X}_i^m(\vec{q}_k^{\,i})$. Then we define

$$\begin{aligned}\underline{\widehat{V}}^h(\Gamma^m) &:= \{\vec{\chi} \in \overset{I_S}{\underset{i=1}{\times}} C(\Gamma_i^m, \mathbb{R}^3) : \vec{\chi}_i|_{\sigma_j^{m,i}} \text{ is linear } \forall\ j = 1 \to J_i,\ i = 1 \to I_S\} \\ &=: [\widehat{W}^h(\Gamma^m)]^3\,,\end{aligned} \tag{3.3}$$

where $\widehat{W}^h(\Gamma^m) \subset \overset{I_S}{\underset{i=1}{\times}} H^1(\Gamma_i^m, \mathbb{R})$ is the space of scalar continuous piecewise linear functions on Γ^m, with $\{\{\phi_k^{m,i}\}_{k=1}^{K_i}\}_{i=1}^{I_S}$ denoting the standard basis of $\widehat{W}^h(\Gamma^m)$, i.e. $\phi_l^{m,i}(\vec{q}_k^{\,m,i}) = \delta_{kl}$ for all $k, l = 1 \to K_i$, $i = 1 \to I_S$. Then $\underline{V}^h(\Gamma^m)$ and $W^h(\Gamma^m)$, the natural discrete analogues of $\underline{V}(\Gamma)$ and $W(\Gamma)$, are defined by

$$\underline{V}^h(\Gamma^m) := \{\vec{\chi} \in \underline{\widehat{V}}^h(\Gamma^m) : \vec{\chi}_{s_1^k} = \vec{\chi}_{s_2^k} = \vec{\chi}_{s_3^k} \text{ on } \mathcal{T}_k^m, \quad k = 1 \to I_T\} \tag{3.4a}$$

$$\text{and} \quad W^h(\Gamma^m) := \{\chi \in \widehat{W}^h(\Gamma^m) : \sum_{j=1}^{3} o_j^k\, \chi_{s_j^k} = 0 \text{ on } \mathcal{T}_k^m, \quad k = 1 \to I_T\}\,. \tag{3.4b}$$

We note that the above definitions imply that $\vec{X}^m = \vec{\mathrm{id}}\,|_{\Gamma^m} \in \underline{V}^h(\Gamma^m)$ on Γ^m and that, if $\vec{X}^{m+1} \in \underline{V}^h(\Gamma^m)$, then $\Gamma^{m+1} = \vec{X}^{m+1}(\Gamma^m)$ can be parameterized with a function from $\underline{V}^h(\Omega^h)$, which we will also denote by $\vec{X}^{m+1}$.

Similarly to (1.7), we introduce the L^2 inner product $\langle\cdot,\cdot\rangle_m$ over the current polyhedral surface cluster Γ^m, which is described by the vector function $\vec{X}^m$, as follows

$$\langle u, v\rangle_m := \sum_{i=1}^{I_S} \int_{\Gamma_i^m} u_i \,.\, v_i \,\mathrm{d}\mathcal{H}^2.$$

If u, v are piecewise continuous, with possible jumps across the edges of $\{\sigma_j^{m,i}\}_{j=1}^{J_i}$, $i = 1 \to I_S$, we introduce the mass lumped inner product $\langle\cdot,\cdot\rangle_m^h$ as

$$\langle u, v\rangle_m^h := \sum_{i=1}^{I_S} \tfrac{1}{3} \sum_{j=1}^{J_i} |\sigma_j^{m,i}| \sum_{k=0}^{2} \lim_{\sigma_j^{m,i} \ni \vec{p} \to \vec{q}_{j_k}^{\,m,i}} (u_i \,.\, v_i)(\vec{p})\,,$$

where $\{\vec{q}_{j_k}^{\,m,i}\}_{k=0}^2$ are the vertices of $\sigma_j^{m,i}$. Here $|\sigma_j^{m,i}| = \frac{1}{2}\,|(\vec{q}_{j_1}^{\,m,i} - \vec{q}_{j_0}^{\,m,i}) \wedge (\vec{q}_{j_2}^{\,m,i} - \vec{q}_{j_0}^{\,m,i})|$ is the measure of $\sigma_j^{m,i}$. In addition, we introduce the unit normal $\vec{\nu}_i^m$ to Γ_i^m; that is,

$$\vec{\nu}_{i,j}^{\,m} := \vec{\nu}_i^m\,|_{\sigma_j^{m,i}} := \frac{(\vec{q}_{j_1}^{\,m,i} - \vec{q}_{j_0}^{\,m,i}) \wedge (\vec{q}_{j_2}^{\,m,i} - \vec{q}_{j_0}^{\,m,i})}{|(\vec{q}_{j_1}^{\,m,i} - \vec{q}_{j_0}^{\,m,i}) \wedge (\vec{q}_{j_2}^{\,m,i}) - \vec{q}_{j_0}^{\,m,i})|}\,,$$

where we have assumed that the vertices $\{\vec{q}_{j_k}^{\,m,i}\}_{k=0}^2$ are ordered with the same orientation for all $\sigma_j^{m,i}$, $j = 1 \to J_i$. Finally, we set $|\cdot|_m^2 := \langle\cdot,\cdot\rangle_m$ and $|\cdot|_{m,h}^2 := \langle\cdot,\cdot\rangle_m^h$.

Then we introduce the following parametric finite element approximations of (1.10a,b) and (1.11a,b). Find $\vec{X}^{m+1} \in \underline{V}^h(\Gamma^m)$ and $\kappa^{m+1} \in \widehat{W}^h(\Gamma^m)$ such that

$$\langle \frac{\vec{X}^{m+1} - \vec{X}^m}{\tau_m}, \chi\,\vec{\nu}^m\rangle_m^h - \langle \kappa^{m+1}, \chi\rangle_m^h = 0 \qquad \forall\ \chi \in \widehat{W}^h(\Gamma^m), \tag{3.5a}$$

$$\langle \kappa^{m+1}\,\vec{\nu}^m, \vec{\eta}\rangle_m^h + \langle \nabla_s\,\vec{X}^{m+1}, \nabla_s\,\vec{\eta}\rangle_m = 0 \qquad \forall\ \vec{\eta} \in \underline{V}^h(\Gamma^m). \tag{3.5b}$$

Find $\vec{X}^{m+1} \in \underline{V}^h(\Gamma^m)$ and $\kappa^{m+1} \in W^h(\Gamma^m)$ such that

$$\langle \frac{\vec{X}^{m+1} - \vec{X}^m}{\tau_m}, \chi\,\vec{\nu}^m\rangle_m^h - \langle \nabla_s\,\kappa^{m+1}, \nabla_s\,\chi\rangle_m = 0 \qquad \forall\ \chi \in W^h(\Gamma^m), \tag{3.6a}$$

$$\langle \kappa^{m+1}\,\vec{\nu}^m, \vec{\eta}\rangle_m^h + \langle \nabla_s\,\vec{X}^{m+1}, \nabla_s\,\vec{\eta}\rangle_m = 0 \qquad \forall\ \vec{\eta} \in \underline{V}^h(\Gamma^m). \tag{3.6b}$$

Following the novel approximations introduced in Barrett, Garcke, and Nürnberg (2008c), we can generalize the above schemes to their anisotropic counter parts. On recalling (1.22a,b) and (1.23a,b) we introduce the following fully practical parametric finite element approximations. Find $\vec{X}^{m+1} \in \underline{V}^h(\Gamma^m)$ and $\kappa_\gamma^{m+1} \in \widehat{W}^h(\Gamma^m)$ such that

$$\langle \frac{\vec{X}^{m+1} - \vec{X}^m}{\tau_m}, \chi\,\vec{\nu}^m\rangle_m^h - \langle \beta(\vec{\nu}^m)\,\kappa_\gamma^{m+1}, \chi\rangle_m^h = 0 \qquad \forall\ \chi \in \widehat{W}^h(\Gamma^m), \tag{3.7a}$$

$$\langle \kappa_\gamma^{m+1}\,\vec{\nu}^m, \vec{\eta}\rangle_m^h + \langle \nabla_s^{\widetilde{G}}\,\vec{X}^{m+1}, \nabla_s^{\widetilde{G}}\,\vec{\eta}\rangle_{\gamma,m} = 0 \qquad \forall\ \vec{\eta} \in \underline{V}^h(\Gamma^m). \tag{3.7b}$$

Find $\vec{X}^{m+1} \in \underline{V}^h(\Gamma^m)$ and $\kappa_\gamma^{m+1} \in W^h(\Gamma^m)$ such that

$$\langle \frac{\vec{X}^{m+1} - \vec{X}^m}{\tau_m}, \chi\, \vec{\nu}^m \rangle_m^h - \langle \beta(\vec{\nu}^m)\, \nabla_s\, \kappa_\gamma^{m+1}, \nabla_s\, \chi \rangle_m = 0 \qquad \forall\ \chi \in W^h(\Gamma^m), \tag{3.8a}$$

$$\langle \kappa_\gamma^{m+1}\, \vec{\nu}^m, \vec{\eta} \rangle_m^h + \langle \nabla_s^{\widetilde{G}}\, \vec{X}^{m+1}, \nabla_s^{\widetilde{G}}\, \vec{\eta} \rangle_{\gamma,m} = 0 \qquad \forall\ \vec{\eta} \in \underline{V}^h(\Gamma^m). \tag{3.8b}$$

Here $\langle \nabla_s^{\widetilde{G}} \cdot, \nabla_s^{\widetilde{G}} \cdot \rangle_{\gamma,m}$ is the discrete inner product defined by

$$\langle \nabla_s^{\widetilde{G}}\, \vec{\eta}, \nabla_s^{\widetilde{G}}\, \vec{\chi} \rangle_{\gamma,m} := \sum_{i=1}^{I_S} \sum_{\ell=1}^{L_i} \int_{\Gamma_i^m} \left[\frac{\gamma_i^{(\ell)}(\vec{\nu}_i^{m+1})}{\gamma_i(\vec{\nu}_i^{m+1})} \right]^{r_i - 1} (\nabla_s^{\widetilde{G}_i^{(\ell)}}\, \vec{\eta}_i, \nabla_s^{\widetilde{G}_i^{(\ell)}}\, \vec{\chi}_i)_{\widetilde{G}_i^{(\ell)}}\, \gamma_i^{(\ell)}(\vec{\nu}_i^m)\, \mathrm{d}\mathcal{H}^2\,. \tag{3.9}$$

Note that (3.9) is a natural discrete analogue of (1.24a), see Barrett, Garcke, and Nürnberg (2008c) for details. The particular choice of normals from the old surface cluster, Γ^m, and the new cluster, Γ^{m+1}, ensures that the solutions to (3.7a,b) and (3.8a,b) are unconditionally stable; see Theorem 3.2, below. Note that this particular choice leads in general to a nonlinear system for $(\vec{X}^{m+1}, \kappa_\gamma^{m+1})$. However, the simpler case $r = (1, \ldots, 1)$ leads to a linear system for $(\vec{X}^{m+1}, \kappa_\gamma^{m+1})$. Finally, observe that in the isotropic case, $\gamma = (|\cdot|, \ldots, |\cdot|)$, the anisotropic schemes above collapse to their isotropic equivalents (3.5a,b) and (3.6a,b), respectively.

Finally, the schemes (3.7a,b) and (3.8a,b) can easily be extended to the case when boundary intersections are present. Let $\partial\mathcal{D}$ be given by a function $F \in C^1(\mathbb{R}^3)$ such that

$$\partial\mathcal{D} = \{\vec{z} \in \mathbb{R}^3 : F(\vec{z}) = 0\} \qquad \text{and} \qquad |\nabla F(\vec{z})| = 1 \quad \forall\ \vec{z} \in \partial\mathcal{D}\,,$$

and let the discrete analogue of $\underline{V}_\partial(\Gamma)$ be defined as

$$\underline{V}_\partial^h(\Gamma^m) := \{\vec{\chi} \in \underline{V}^h(\Gamma^m) : \nabla F(\vec{q})\,.\,\vec{\chi}_{s_k}(\vec{q}) = 0 \quad \forall\ \vec{q} \in \mathcal{B}_k^m\,, \quad k = 1 \to I_B\}\,,$$

where $\mathcal{B}_k^m := \{\vec{q}_l^{\,m,s_k}\}_{l=1}^{K_{s_k}} \cap \vec{X}_{s_k}^m(\partial_{p_k}\Omega_{s_k}^h)$. Then we introduce the following approximations. Find $\delta\vec{X}^{m+1} \in \underline{V}_\partial^h(\Gamma^m)$ and $\kappa_\gamma^{m+1} \in \widehat{W}^h(\Gamma^m)$, where $\vec{X}^{m+1} := \vec{X}^m + \delta\vec{X}^{m+1}$, such that

$$\langle \frac{\delta\vec{X}^{m+1}}{\tau_m}, \chi\, \vec{\nu}^m \rangle_m^h - \langle \beta(\vec{\nu}^m)\, \kappa_\gamma^{m+1}, \chi \rangle_m^h = 0 \qquad \forall\ \chi \in \widehat{W}^h(\Gamma^m), \tag{3.10a}$$

$$\langle \kappa_\gamma^{m+1}\, \vec{\nu}^m, \vec{\eta} \rangle_m^h + \langle \nabla_s^{\widetilde{G}}\, \vec{X}^{m+1}, \nabla_s^{\widetilde{G}}\, \vec{\eta} \rangle_{\gamma,m} = 0 \qquad \forall\ \vec{\eta} \in \underline{V}_\partial^h(\Gamma^m)\,. \tag{3.10b}$$

Find $\delta\vec{X}^{m+1} \in \underline{V}_\partial^h(\Gamma^m)$ and $\kappa_\gamma^{m+1} \in W^h(\Gamma^m)$, where $\vec{X}^{m+1} := \vec{X}^m + \delta\vec{X}^{m+1}$, such that

$$\langle \frac{\delta\vec{X}^{m+1}}{\tau_m}, \chi\, \vec{\nu}^m \rangle_m^h - \langle \beta(\vec{\nu}^m)\, \nabla_s\, \kappa_\gamma^{m+1}, \nabla_s\, \chi \rangle_m = 0 \qquad \forall\ \chi \in W^h(\Gamma^m), \tag{3.11a}$$

$$\langle \kappa_\gamma^{m+1}\, \vec{\nu}^m, \vec{\eta} \rangle_m^h + \langle \nabla_s^{\widetilde{G}}\, \vec{X}^{m+1}, \nabla_s^{\widetilde{G}}\, \vec{\eta} \rangle_{\gamma,m} = 0 \qquad \forall\ \vec{\eta} \in \underline{V}_\partial^h(\Gamma^m)\,. \tag{3.11b}$$

We note that the constraint $\delta\vec{X}^{m+1} \in \underline{V}_\partial^h(\Gamma^m)$ weakly approximates (1.25), as it is a linearized approximation of these constraints. In particular, for curved boundaries $\partial\mathcal{D}$ the equations

$$F(\vec{X}_{s_k}^{m+1}) = 0 \quad \text{on } \partial_{p_k}\Omega_{s_k}^h, \qquad k = 1 \to I_B\,, \tag{3.12}$$

are only approximately satisfied, see e.g. Barrett, Garcke, and Nürnberg (2007b) for more details in the planar isotropic case. As a remedy, one could employ a projection step that orthogonally projects $\vec{X}^{m+1}$ onto $\partial\mathcal{D}$ at every time step, which would have the advantage of satisfying (3.12) exactly throughout the evolution. But in general this would result in a loss of our stability bound, see Theorem 3.4 below; hence our preference for the stated approximations.

On noting that $\underline{V}^h_\partial(\Gamma^m) \equiv \underline{V}^h(\Gamma^m)$ if $I_B = 0$, it follows that the schemes (3.10a,b) and (3.11a,b) collapse to (3.7a,b) and (3.8a,b) in this case.

Before we can proceed to prove existence and uniqueness to these approximations, we have to make the following very mild assumption on the triangulations at each time level.

($\mathcal{A}$) We assume for $m = 0 \to M$ and for $i = 1 \to I_S$ that $|\det[D\vec{X}^m_i]^T\,[D\vec{X}^m_i]| > 0$ almost everywhere in Ω^h_i, so that $|\sigma^{m,i}_j| = |\vec{X}^m_i(\sigma^i_j)| > 0$, $j = 1 \to J_i$.

For $k = 1 \to K_i$, let $\Xi^{m,i}_k := \{\sigma^{m,i}_j : \vec{q}^{\,m,i}_k \in \overline{\sigma^{m,i}_j}\}$ and set

$$\Lambda^{m,i}_k := \bigcup_{\sigma^{m,i}_j \in \Xi^{m,i}_k} \overline{\sigma^{m,i}_j} \qquad \text{and} \qquad \vec{\omega}^m_{i,k} := \frac{1}{|\Lambda^{m,i}_k|} \sum_{\sigma^i_j \in \Xi^{m,i}_k} |\sigma^{m,i}_j|\,\vec{\nu}^m_{i,j}\,.$$

Then we assume further that for each $i = 1 \to I_S$ there exists a $k \in \{1, \dots, \overline{K}_i\}$ such that $\vec{\omega}^m_{i,k} \neq \vec{0}$. Moreover, we require that $\dim \operatorname{span}\{\{\vec{\omega}^m_{i,k}\}_{k=1}^{\overline{K}_i}\}_{i=1}^{I_S} = 3$, $m = 0 \to M-1$.

THEOREM. 3.1. *Let the assumption* ($\mathcal{A}$) *hold. Then there exist unique solutions* $(\vec{X}^{m+1}, \kappa^{m+1}) \in \underline{V}^h(\Gamma^m) \times \widehat{W}^h(\Gamma^m)$ *to the system* (3.5a,b)*; and* $(\vec{X}^{m+1}, \kappa^{m+1}) \in \underline{V}^h(\Gamma^m) \times W^h(\Gamma^m)$ *to* (3.6a,b)*.*

Proof. This follows directly from Theorem 3.3, below. □

THEOREM. 3.2. *Let the assumptions* ($\mathcal{A}$) *hold, and* $\{(\vec{X}^m, \kappa^m)\}_{m=1}^M$ *be the unique solution to* (3.6a,b)*. Then for* $k = 1 \to M$ *we have that*

$$|\Gamma^k| + \sum_{m=0}^{k-1} \tau_m\,|\nabla_s\,\kappa^{m+1}|^2_m \leq |\Gamma^0|\,. \tag{3.13a}$$

Similarly, the unique solution to (3.5a,b) *satisfies for* $k = 1 \to M$

$$|\Gamma^k| + \sum_{m=0}^{k-1} \tau_m\,|\kappa^{m+1}|^2_{m,h} \leq |\Gamma^0|\,. \tag{3.13b}$$

Proof. Clearly, the result directly follows from Theorem 3.4, below. For the benefit of the reader, we also give a separate proof for the isotropic case. We first consider (3.13a). Choosing $\chi = \kappa^{m+1} \in W^h(\Gamma^m)$ in (3.6a) and $\vec{\eta} = \frac{\vec{X}^{m+1} - \vec{X}^m}{\tau_m} \in \underline{V}^h(\Gamma^m)$ in (3.6b) yields that

$$\langle \nabla_s\,\vec{X}^{m+1}, \nabla_s\,(\vec{X}^{m+1} - \vec{X}^m)\rangle_m + \tau_m\,|\nabla_s\,\kappa^{m+1}|^2_m = 0\,. \tag{3.14}$$

It follows from Lemma 2.1 in Barrett, Garcke, and Nürnberg (2008b), on noting that $\vec{X}^m \equiv \vec{\mathrm{id}}$ on Γ^m, that

$$\begin{aligned}\langle \nabla_s \vec{X}^{m+1}, \nabla_s (\vec{X}^{m+1} - \vec{X}^m)\rangle_m &= \tfrac{1}{2}\left[|\nabla_s \vec{X}^{m+1}|_m^2 - |\nabla_s \vec{X}^m|_m^2 + |\nabla_s (\vec{X}^{m+1} - \vec{X}^m)|_m^2\right] \\ &\geq |\Gamma^{m+1}| - |\Gamma^m| + \tfrac{1}{2}\,|\nabla_s (\vec{X}^{m+1} - \vec{X}^m)|_m^2\,. \end{aligned} \tag{3.15}$$

Combining (3.14) and (3.15) yields that

$$|\Gamma^{m+1}| - |\Gamma^m| + \tau_m\,|\nabla_s\,\kappa^{m+1}|_m^2 + \tfrac{1}{2}|\nabla_s (\vec{X}^{m+1} - \vec{X}^m)|_m^2 \leq 0\,. \tag{3.16}$$

Summing (3.16) for $m = 0 \to k-1$ yields the desired result. The steps of the proof of (3.13b) are exactly the same. ☐

THEOREM. 3.3. *Let the assumption* $(\mathcal{A})$ *hold and let* $r = (1, \ldots, 1)$. *Then there exist unique solutions* $(\vec{X}^{m+1}, \kappa_\gamma^{m+1}) \in \underline{V}^h(\Gamma^m) \times \widehat{W}^h(\Gamma^m)$ *to the system* (3.7a,b)*; and* $(\vec{X}^{m+1}, \kappa_\gamma^{m+1}) \in \underline{V}^h(\Gamma^m) \times W^h(\Gamma^m)$ *to* (3.8a,b). *Moreover, there exist unique solutions* $(\delta\vec{X}^{m+1}, \kappa_\gamma^{m+1}) \in \underline{V}_\partial^h(\Gamma^m) \times \widehat{W}^h(\Gamma^m)$ *to the system* (3.10a,b)*; and* $(\delta\vec{X}^{m+1}, \kappa_\gamma^{m+1}) \in \underline{V}_\partial^h(\Gamma^m) \times W^h(\Gamma^m)$ *to* (3.11a,b).

Proof. As (3.7a,b) is linear, existence follows from uniqueness. To investigate the latter, we consider the system: Find $\{\vec{X}, \kappa_\gamma\} \in \underline{V}^h(\Gamma^m) \times \widehat{W}^h(\Gamma^m)$ such that

$$\langle \vec{X}, \chi\,\vec{\nu}^m\rangle_m^h - \tau_m\,\langle \beta(\vec{\nu}^m)\,\kappa_\gamma, \chi\rangle_m^h = 0 \quad \forall\ \chi \in \widehat{W}^h(\Gamma^m), \tag{3.17a}$$

$$\langle \kappa_\gamma\,\vec{\nu}^m, \vec{\eta}\rangle_m^h + \sum_{i=1}^{I_S}\sum_{\ell=1}^{L_i}\int_{\Gamma_i^m} (\nabla_s^{\widetilde{G}_i^{(\ell)}}\,\vec{X}_i, \nabla_s^{\widetilde{G}_i^{(\ell)}}\,\vec{\eta}_i)_{\widetilde{G}_i^{(\ell)}}\,\gamma_i^{(\ell)}(\vec{\nu}_i^m)\ \mathrm{d}\mathcal{H}^2 = 0 \quad \forall\ \vec{\eta} \in \underline{V}^h(\Gamma^m)\,. \tag{3.17b}$$

Choosing $\chi = \kappa_\gamma \in \widehat{W}^h(\Gamma^m)$ in (3.17a) and $\vec{\eta} = \vec{X} \in \underline{V}^h(\Gamma^m)$ in (3.17b) yields that

$$\sum_{i=1}^{I_S}\sum_{\ell=1}^{L_i}\int_{\Gamma_i^m} (\nabla_s^{\widetilde{G}_i^{(\ell)}}\,\vec{X}_i, \nabla_s^{\widetilde{G}_i^{(\ell)}}\,\vec{X}_i)_{\widetilde{G}_i^{(\ell)}}\,\gamma_i^{(\ell)}(\vec{\nu}_i^m)\ \mathrm{d}\mathcal{H}^2 + \tau_m\,\langle \beta(\vec{\nu}^m)\,\kappa_\gamma, \kappa_\gamma\rangle_m^h = 0\,. \tag{3.18}$$

It follows from (3.18), (1.24b), the positive definiteness of $\widetilde{G}_i^{(\ell)}$, $\ell = 1 \to L_i$, $i = 1 \to I_S$, and the positivity of β that $\kappa_\gamma = (0, \ldots, 0)$ and, on noting $\vec{X} \in \underline{V}^h(\Gamma^m)$ and the connectedness of Γ^m, that $\vec{X}_i \equiv \vec{X}^c \in \mathbb{R}^3$, $i = 1 \to I_S$. Hence it follows that

$$\langle \vec{X}^c, \chi\,\vec{\nu}^m\rangle_m^h = 0 \quad \forall\ \chi \in \widehat{W}^h(\Gamma^m)\,. \tag{3.19}$$

Choosing $\chi = (0, \ldots, 0, \phi_k^{m,i}, 0, \ldots, 0)$ in (3.19) yields that $\vec{X}^c\,.\,\vec{\omega}_{i,k}^m = 0$ for $k = 1 \to \overline{K}_i$, $i = 1 \to I_S$. It follows from assumption $(\mathcal{A})$ that $\vec{X}^c = \vec{0}$. Hence we have shown that there exists a unique solution $(\vec{X}^{m+1}, \kappa_\gamma^{m+1}) \in \underline{V}^h(\Gamma^m) \times \widehat{W}^h(\Gamma^m)$ to (3.7a,b).

The corresponding proof for the system (3.8a,b) is similar with only a minor modification. In particular, following the same argument we obtain (3.18) with the second term replaced by $\tau_m \langle \beta(\vec{\nu}^m) \nabla_s \kappa_\gamma, \nabla_s \kappa_\gamma \rangle_m$, which implies that $\kappa_{\gamma,i} \equiv \kappa_i^c \in \mathbb{R}$ and $\vec{X}_i \equiv \vec{X}^c \in \mathbb{R}^3$, $i = 1 \to I_S$. Hence

$$\langle \kappa^c \, \vec{\nu}^m, \vec{\eta} \rangle_m^h = 0 \quad \forall \, \vec{\eta} \in \underline{V}^h(\Gamma^m) \,. \tag{3.20}$$

For a fixed $i = 1 \to I_S$, choosing $\vec{\eta} = (0, \ldots, 0, \vec{z}\, \phi_k^{m,i}, 0, \ldots, 0)$, $k = 1 \to \overline{K}_i$, in (3.20) yields, on assuming $\kappa_i^c \neq 0$, that for $k = 1 \to \overline{K}_i$

$$\vec{\omega}_{i,k}^m \,.\, \vec{z} = 0 \quad \forall \, \vec{z} \in \mathbb{R}^3 \qquad \Longleftrightarrow \qquad \vec{\omega}_{i,k}^m = \vec{0}.$$

However, this contradicts assumption $(\mathcal{A})$ and hence $\kappa_i^c = 0$, $i = 1 \to I_S$, i.e. $\kappa_\gamma = (0, \ldots, 0)$. Now $\vec{X} = (\vec{0}, \ldots, \vec{0})$ follows as before, and so there exists a unique solution $(\vec{X}^{m+1}, \kappa_\gamma^{m+1}) \in \underline{V}^h(\Gamma^m) \times W^h(\Gamma^m)$ to (3.8a,b).

Finally, the proofs for (3.10a,b) and (3.11a,b) are identical with $\underline{V}^h(\Gamma^m)$ replaced by $\underline{V}_\partial^h(\Gamma^m)$. ∎

THEOREM. 3.4. *Let the assumptions* $(\mathcal{A})$ *hold, and let* $\{(\vec{X}^m, \kappa_\gamma^m)\}_{m=1}^M$ *be a solution to* (3.8a,b) *or* (3.11a,b). *Then for* $k = 1 \to M$ *we have that*

$$|\Gamma^k|_\gamma + \sum_{m=0}^{k-1} \tau_m \, \langle \beta(\vec{\nu}^m) \, \nabla_s \, \kappa_\gamma^{m+1}, \nabla_s \, \kappa_\gamma^{m+1} \rangle_m \leq |\Gamma^0|_\gamma \,. \tag{3.21a}$$

Similarly, the solutions to (3.7a,b) *and* (3.10a,b) *satisfies for* $k = 1 \to M$

$$|\Gamma^k|_\gamma + \sum_{m=0}^{k-1} \tau_m \, \langle \beta(\vec{\nu}^m) \, \kappa_\gamma^{m+1}, \kappa_\gamma^{m+1} \rangle_m^h \leq |\Gamma^0|_\gamma \,. \tag{3.21b}$$

Proof. As the four proofs are almost identical, it is sufficient to show (3.21a) for the approximation (3.8a,b). Choosing $\chi = \kappa_\gamma^{m+1} \in W^h(\Gamma^m)$ in (3.8a) and $\vec{\eta} = \frac{\vec{X}^{m+1} - \vec{X}^m}{\tau_m} \in \underline{V}^h(\Gamma^m)$ in (3.8b) yields that

$$\langle \nabla_s \, \vec{X}^{m+1}, \nabla_s \, (\vec{X}^{m+1} - \vec{X}^m) \rangle_{\gamma,m} + \tau_m \, \langle \beta(\vec{\nu}^m) \, \nabla_s \, \kappa_\gamma^{m+1}, \nabla_s \, \kappa_\gamma^{m+1} \rangle_m = 0 \,. \tag{3.22}$$

It follows from Barrett, Garcke, and Nürnberg (2008c, Lemma 3.1), similarly to the proof of Theorem 3.2 in Barrett, Garcke, and Nürnberg (2008c), on noting that $\vec{X}^m \equiv \vec{\mathrm{id}}$ on Γ^m, that

$$\langle \nabla_s^{\widetilde{G}} \, \vec{X}^{m+1}, \nabla_s^{\widetilde{G}} \, (\vec{X}^{m+1} - \vec{X}^m) \rangle_{\gamma,m} \geq |\Gamma^{m+1}|_\gamma - |\Gamma^m|_\gamma \,. \tag{3.23}$$

Combining (3.22) and (3.23) yields that

$$|\Gamma^{m+1}|_\gamma - |\Gamma^m|_\gamma + \tau_m \, \langle \beta(\vec{\nu}^m) \, \nabla_s \, \kappa_\gamma^{m+1}, \nabla_s \, \kappa_\gamma^{m+1} \rangle_m \leq 0 \,. \tag{3.24}$$

Summing (3.24) for $m = 0 \to k - 1$ yields the desired result (3.21a). ∎

REMARK. 3.1. *Similarly to the semidiscrete approximations considered in e.g. Barrett, Garcke, and Nürnberg (2008b,c), it is possible to derive certain properties for semidiscrete versions of the finite element approximations considered in this paper. In particular, one can show that semidiscrete continuous in time variants of our schemes maintain "good mesh properties"; see Barrett, Garcke, and Nürnberg (2008b) for details. Moreover, the semidiscrete versions of* (3.6a,b) *and* (3.8a,b) *maintain the enclosed volumes exactly. To illustrate this, we use the same example as in Remark 2.1 and obtain, on choosing* $\chi = (1,-1,0) \in W^h(\Gamma^m)$ *in the semidiscrete version of* (3.8a)*, where all integration is over the current cluster* $\Gamma^h(t)$*, parameterized by* $\vec{X}(t) \in \underline{V}^h(\Omega^h)$*, with normals* $\vec{\nu}^h$*, that*

$$0 = \int_{\Gamma_1^h} [\vec{X}_1]_t \,.\, \vec{\nu}_1^h \,\mathrm{d}\mathcal{H}^2 - \int_{\Gamma_2^h} [\vec{X}_2]_t \,.\, \vec{\nu}_2^h \,\mathrm{d}\mathcal{H}^2 = \frac{\mathrm{d}}{\mathrm{d}t}\,\mathcal{L}^3(v^h)\,,$$

where v^h *denotes the volume enclosed by the two polyhedral surfaces* Γ_1^h *and* Γ_2^h*. We remark that in practice these properties are (approximately) inherited by our fully discrete schemes. As a result, no heuristic redistribution of mesh points is necessary in practice. Moreover, in all of our numerical experiments, the maximum observed relative volume loss for* (3.6a,b) *and* (3.8a,b) *was always less than* 1%*.*

4 Solution of the discrete systems

For sake of brevity, we only present the details of the solution methods for the isotropic approximations (3.5a,b) and (3.6a,b). They naturally generalize to the appropriate solvers for the anisotropic schemes (3.7a,b), (3.8a,b), (3.10a,b) and (3.11a,b).

Let $K := \sum_{i=1}^{I_S} K_i$ and, for later reference, $J := \sum_{i=1}^{I_S} J_i$. In addition, for any number $n \in \mathbb{N}$, let $Id_n \in \mathbb{R}^{n\times n}$ be the identity matrix, and similarly for $\vec{Id}_n \in (\mathbb{R}^{d\times d})^{n\times n}$. We define the orthogonal projection $\vec{\mathcal{P}} : (\mathbb{R}^3)^K \to \underline{\mathbb{X}}$ onto the Euclidean space associated with $\underline{V}^h(\Gamma^m)$, and similarly $\mathcal{K} : \mathbb{R}^K \to \mathbb{X}$ the orthogonal projection onto the Euclidean space associated with $W^h(\Gamma^m)$. In particular, we have that

$$\vec{\mathcal{P}} = \vec{Id}_K - \vec{\mathcal{Q}}\,\vec{\mathcal{Q}}^T \qquad \text{and} \qquad \mathcal{K} = Id_K - Q\,Q^T\,, \tag{4.1}$$

where the columns of $\vec{\mathcal{Q}}$ and Q form an orthonormal basis of the orthogonal complements $\underline{\mathbb{X}}^\perp$ in $(\mathbb{R}^3)^K$ and $\mathbb{X}^\perp$ in $\mathbb{R}^K$, respectively. The two projections $\mathcal{K}$ and $\vec{\mathcal{P}}$ will be crucial in the construction of fully practical solution methods for the finite element approximations introduced in Section 3. For instance, with the help of these two projections it will be sufficient throughout to work with the bases of the simple product finite element spaces $\widehat{W}^h(\Gamma^m)$ and $\underline{\widehat{V}}^h(\Gamma^m)$, recall (3.3), rather than having to work with the highly nontrivial trial and test spaces $W^h(\Gamma^m)$ and $\underline{V}^h(\Gamma^m)$ directly. This construction is similar to e.g. the standard technique used for an ODE with periodic boundary conditions. The analogous approach by the authors for the treatment of the evolution of curve networks in the plane can be found in e.g. Barrett, Garcke, and Nürnberg (2007a).

REMARK. 4.1. *Before we introduce the linear systems satisfied by the coefficient vectors of our finite element solutions, where we note that the nonlinear approximations will be*

iteratively solved with the help of linear auxiliary problems, we remark on some practical issues related to the crucial projections $\mathcal{K}$ and $\vec{\mathcal{P}}$.

A valid strategy for the computation of e.g. $\vec{\mathcal{P}}$, recall (4.1)*, is to construct the columns of $\vec{\mathcal{Q}}$ directly by finding an orthonormal basis of $\underline{\mathbb{X}}^{\perp}$. This can be achieved for instance by starting with a set of not necessarily linearly independent vectors that span $\underline{\mathbb{X}}^{\perp}$ and then performing an orthogonalization procedure such as Gram–Schmidt. A possible set of such spanning vectors can be easily found on recalling* (3.4a)*, and one advantage of this strategy is that no explicit a priori knowledge about the location of possible quadruple junction points is needed.*

However, this approach soon becomes very inefficient, as the matrix $\vec{\mathcal{Q}}$ can be large in practice. On recalling (3.2) *we note that the number of columns in $\vec{\mathcal{Q}}$ will be close to $6\,Z$, where $Z := \sum_{k=1}^{I_T} Z_k$. In fact, if $I_{QJ} \geq 0$ denotes the number of quadruple junction points, then one can show that $\dim(\underline{\mathbb{X}}^{\perp}) = 6\,Z - 9\,I_{QJ}$. For example, for the experiment in Figure 13 below, we have $6\,Z = 1584$ and $\dim(\underline{\mathbb{X}}^{\perp}) = 6\,Z - 36 = 1548$, while $3\,K = 21915$, meaning that $\vec{\mathcal{Q}}$ is a 21915×1548 matrix. Clearly, computing and applying the projection $\vec{\mathcal{P}}$ in this way is computationally expensive, especially because these projections have to be evaluated many times during the course of employed iterative solution methods; see §4.1 below.*

A better and far more efficient treatment is the following, where we assume that information about the I_{QJ} quadruple junction points and their location is available. In particular, we assume that for each quadruple junction point we are given a quadruple (j_1, j_2, j_3, j_4) identifying the four triple junction lines $\mathcal{T}_{j_i}$, $i = 1 \to 4$, that meet there. In addition, for the discretizations we are given for each line $\mathcal{T}_{j_i}$ the index l_{j_i} such that $\vec{X}^m_{s_k^{j_i}}(\vec{\rho}_k^{\,j_i}(l_{j_i}))$, $k = 1 \to 3$, is the quadruple junction point of Γ^m at which the discretizations $\mathcal{T}^m_{j_i}$ of $\mathcal{T}_{j_i}$, $i = 1 \to 4$, meet; recall (3.4a)*. It is not difficult to see that the action of $\vec{\mathcal{P}}$ is equivalent to several independent* local *projections, that each involve only very few vertices. In particular, a suitable permutation of its rows and columns transforms $\vec{\mathcal{P}}$ into a block diagonal form, with only three types of blocks on the diagonal. These blocks are*

$$(1)\,, \qquad \tfrac{1}{3}\begin{pmatrix} 1 & 1 & 1 \\ 1 & 1 & 1 \\ 1 & 1 & 1 \end{pmatrix}, \qquad \tfrac{1}{6}\begin{pmatrix} 1 & 1 & 1 & 1 & 1 & 1 \\ 1 & 1 & 1 & 1 & 1 & 1 \\ 1 & 1 & 1 & 1 & 1 & 1 \\ 1 & 1 & 1 & 1 & 1 & 1 \\ 1 & 1 & 1 & 1 & 1 & 1 \\ 1 & 1 & 1 & 1 & 1 & 1 \end{pmatrix}, \tag{4.2}$$

for vertices lying in the interior of a surface, vertices on a triple junction line that do not correspond to quadruple junction points and vertices that correspond to quadruple junction points, respectively. For the latter case we note that at a quadruple junction point exactly six distinct surfaces meet. Applying the local projections (4.2) *is now straightforward and very efficient.*

A similar approach can be applied to the projection $\mathcal{K}$. Once again we note that the constraints in (3.4b) *mean that $\mathcal{K}$ is equivalent to several independent local projections. We leave the details to the interested reader but note that in diagonalized form the blocks*

of $\mathcal{K}$ may be of the form e.g.

$$(1)\ , \qquad \tfrac{1}{3}\begin{pmatrix} 2 & -1 & -1 \\ -1 & 2 & -1 \\ -1 & -1 & 2 \end{pmatrix} \tag{4.3a}$$

for vertices lying in the interior of a surface and vertices on a triple junction line, say $\mathcal{T}_k^m$ with $o^k = (1,1,1)$, that do not correspond to quadruple junction points, respectively, and of the form e.g.

$$\tfrac{1}{4}\begin{pmatrix} 2 & 1 & 1 & -1 & 1 & 0 \\ 1 & 2 & 1 & 0 & -1 & 1 \\ 1 & 1 & 2 & 1 & 0 & -1 \\ -1 & 0 & 1 & 2 & -1 & -1 \\ 1 & -1 & 0 & -1 & 2 & -1 \\ 0 & 1 & -1 & -1 & -1 & 2 \end{pmatrix}\ , \qquad \tfrac{1}{8}\begin{pmatrix} 4 & 2 & 2 & -2 & -2 & 0 \\ 2 & 3 & 3 & 1 & 1 & 0 \\ 2 & 3 & 3 & 1 & 1 & 0 \\ -2 & 1 & 1 & 3 & 3 & 0 \\ -2 & 1 & 1 & 3 & 3 & 0 \\ 0 & 0 & 0 & 0 & 0 & 0 \end{pmatrix}\ , \tag{4.3b}$$

for vertices that correspond to quadruple junction points; where similar blocks with slightly different signs are obtained for different choices of (o_1^k, o_2^k, o_3^k), $k = 1 \to I_T$. In particular, the examples in (4.3b) *are induced by the choices*

$$\begin{pmatrix} 1 & 0 & -1 & 1 & 0 & 0 \\ -1 & 1 & 0 & 0 & 1 & 0 \\ 0 & -1 & 1 & 0 & 0 & 1 \\ 0 & 0 & 0 & 1 & 1 & 1 \end{pmatrix} \qquad \textit{and} \qquad \begin{pmatrix} 1 & -1 & 0 & 1 & 0 & 0 \\ 1 & 0 & -1 & 0 & 1 & 0 \\ 0 & 0 & 0 & -1 & 1 & 1 \\ 0 & 1 & -1 & 0 & 0 & 1 \end{pmatrix}$$

for the orientation coefficients o^{j_i}, $i = 1 \to 4$, for the six surfaces meeting at the four triple junction lines, respectively. Similarly to (4.2)*, applying the local projections* (4.3a,b) *is straightforward.*

In order to give a matrix formulation for (3.5a,b) we introduce the matrices $M^i \in \mathbb{R}^{K_i \times K_i}$, $\vec{N}^i \in (\mathbb{R}^3)^{K_i \times K_i}$, $A^i \in \mathbb{R}^{K_i \times K_i}$ and $\vec{A}^i \in (\mathbb{R}^{d\times d})^{K_i \times K_i}$, $i = 1 \to I_S$, defined by

$$\begin{aligned} M_{kl}^i &:= \int_{\Gamma_i^m} \pi_i^m[\phi_k^{m,i}\,\phi_l^{m,i}]\,\mathrm{d}\mathcal{H}^2, \qquad \vec{N}_{kl}^i := \int_{\Gamma_i^m} \pi_i^m[\phi_k^{m,i}\,\phi_l^{m,i}]\,\vec{\nu}_i^m\,\mathrm{d}\mathcal{H}^2, \\ A_{kl}^i &:= \int_{\Gamma_i^m} \nabla_s\,\phi_k^{m,i}\,.\,\nabla_s\,\phi_l^{m,i}\,\mathrm{d}\mathcal{H}^2, \qquad \vec{A}_{kl}^i := A_{kl}^i\,\vec{Id}_1\,, \end{aligned}$$

where we recall that $\{\{\phi_k^{m,i}\}_{k=1}^{K_i}\}_{i=1}^{I_S}$ is the standard basis of $\widehat{W}^h(\Gamma^m)$ and $\pi^m := (\pi_1^m, \ldots, \pi_{I_S}^m) : C(\Gamma^m, \mathbb{R}) \to \widehat{W}^h(\Gamma^m)$ is the standard interpolation operator at the nodes $\{\{\vec{q}_k^{m,i}\}_{k=1}^{K_i}\}_{i=1}^{I_S}$. Then on introducing the matrices

$$\begin{aligned} M &:= \mathrm{diag}(M^1, \ldots, M^{I_S}),\ A := \mathrm{diag}(A^1, \ldots, A^{I_S}), \\ \vec{A} &:= \mathrm{diag}(\vec{A}^1, \ldots, \vec{A}^{I_S}),\ \vec{N} := \mathrm{diag}(\vec{N}^1, \ldots, \vec{N}^{I_S}), \end{aligned}$$

where $M, A : \mathbb{R}^K \to \mathbb{R}^K$, $\vec{A} : (\mathbb{R}^3)^K \to (\mathbb{R}^3)^K$ and $\vec{N} : \mathbb{R}^K \to (\mathbb{R}^3)^K$, the system of equations (3.5a,b) can be written as: Find $(\delta\vec{X}^{m+1}, \kappa^{m+1}) \in \underline{\mathbb{X}} \times \mathbb{R}^K$ such that

$$\begin{pmatrix} M & -\frac{1}{\tau_m}\vec{N}^T\vec{\mathcal{P}} \\ \vec{\mathcal{P}}\vec{N} & \vec{\mathcal{P}}\vec{A}\vec{\mathcal{P}} \end{pmatrix}\begin{pmatrix} \kappa^{m+1} \\ \delta\vec{X}^{m+1} \end{pmatrix} = \begin{pmatrix} 0 \\ -\vec{\mathcal{P}}\vec{A}\vec{\mathcal{P}}\,\vec{X}^m \end{pmatrix}. \tag{4.4}$$

Here, with the obvious abuse of notation, $\kappa^{m+1} = (\kappa_1^{m+1}, \ldots, \kappa_{I_S}^{m+1})^T$ with $\kappa_i^{m+1} = ([\kappa_i^{m+1}]_1, \ldots, [\kappa_i^{m+1}]_{K_i})$, $i = 1 \to I_S$, and $\delta\vec{X}^{m+1} = (\delta\vec{X}_1^{m+1}, \ldots, \delta\vec{X}_{I_S}^{m+1})^T$ with $\delta\vec{X}_i^{m+1} = ([\delta\vec{X}_i^{m+1}]_1, \ldots, [\delta\vec{X}_i^{m+1}]_{K_i})$, $i = 1 \to I_S$, are the vectors of coefficients with respect to the standard basis $\{\{\phi_k^i\}_{k=1}^{K_i}\}_{i=1}^{I_S}$ of κ^{m+1} and $\vec{X}^{m+1} - \vec{X}^m$ in (3.5a,b), respectively.

Similarly, the system (3.6a,b) can be written as: Find $(\delta\vec{X}^{m+1}, \kappa^{m+1}) \in \underline{\mathbb{X}} \times \mathbb{X}$ such that

$$\begin{pmatrix} \mathcal{K}A\mathcal{K} & -\frac{1}{\tau_m}\mathcal{K}\vec{N}^T\vec{\mathcal{P}} \\ \vec{\mathcal{P}}\vec{N}\mathcal{K} & \vec{\mathcal{P}}\vec{A}\vec{\mathcal{P}} \end{pmatrix} \begin{pmatrix} \kappa^{m+1} \\ \delta\vec{X}^{m+1} \end{pmatrix} = \begin{pmatrix} 0 \\ -\vec{\mathcal{P}}\vec{A}\vec{\mathcal{P}}\,\vec{X}^m \end{pmatrix}. \tag{4.5}$$

4.1 Schur complement approach

As M is non-singular, we can reformulate (4.4) as

$$\kappa^{m+1} = \tfrac{1}{\tau_m}\, M^{-1}\, \vec{N}^T\vec{\mathcal{P}}\, \delta\vec{X}^{m+1}, \tag{4.6a}$$

$$(\vec{\mathcal{P}}\vec{A}\vec{\mathcal{P}} + \tfrac{1}{\tau_m}\,\vec{\mathcal{P}}\vec{N}\, M^{-1}\, \vec{N}^T\vec{\mathcal{P}})\, \delta\vec{X}^{m+1} = -\vec{\mathcal{P}}\vec{A}\vec{\mathcal{P}}\,\vec{X}^m. \tag{4.6b}$$

Similarly, (4.5) can be solved by applying a Schur complement approach and then solving for $\delta\vec{X}^{m+1} \in \underline{\mathbb{X}}$:

$$\vec{\Pi}\,\vec{\mathcal{P}}\,(\vec{A} + \tfrac{1}{\tau_m}\,\vec{N}\mathcal{K}\,S\,\mathcal{K}\vec{N}^T)\,\vec{\mathcal{P}}\;\vec{\Pi}\,\delta\vec{X}^{m+1} = -\vec{\Pi}\,\vec{\mathcal{P}}\vec{A}\vec{\mathcal{P}}\,\vec{X}^m. \tag{4.7}$$

Here S is the inverse of $\mathcal{K}A\mathcal{K}$ on the space $(\ker \mathcal{K}A\mathcal{K})^\perp$. Also $\vec{\Pi} : (\mathbb{R}^3)^K \to \mathcal{R}^\perp$ is the orthogonal projection onto $\mathcal{R}^\perp$, where $\mathcal{R} := \operatorname{span}\{\vec{\mathcal{P}}\vec{N}\mathcal{K}\, e_i : i = 1 \to I_{EV}\} \equiv \{\vec{\mathcal{P}}\vec{N}\mathcal{K}\, v : v \in \ker \mathcal{K}A\mathcal{K}\} \subset \underline{\mathbb{X}}$ with $\{e_i\}_{i=1}^{I_{EV}}$ being a basis of the space $E = \ker A \cap \mathbb{X}$. In practice we always found that $I_{EV} = \dim(E)$ is equal to the number of volumes enclosed by the given surface cluster; e.g. $I_{EV} = 2$ for a double bubble, $I_{EV} = 3$ for a triple bubble and so on. This is the natural generalization to surface clusters of the result proved for curve networks in the plane, see Barrett, Garcke, and Nürnberg (2007a).

The Schur complement systems (4.6b) and (4.7) can be solved with a (preconditioned) conjugate gradient solver. Here we used a simple diagonal preconditioner as considered in Barrett, Garcke, and Nürnberg (2008a, p. 314) for the two dimensional case. Where necessary, the solution of $\mathcal{K}A\mathcal{K}\, y = x$ in order to compute $S\, x$ can be obtained with an (inner loop) CG solver without a projection, as the right hand side vector x always satisfies the necessary compatibility condition, i.e. $x \in (\ker \mathcal{K}A\mathcal{K})^\perp$. See Hestenes (1975) for a justification of using a CG solver for a positive semidefinite system.

4.2 Anisotropic schemes

In the case $r = (1, \ldots, 1)$, when the approximations (3.7a,b) and (3.8a,b) are linear, the anisotropic equivalents of (4.4) and (4.5) are given by

$$\begin{pmatrix} M_\beta & -\frac{1}{\tau_m}\vec{N}^T\vec{\mathcal{P}} \\ \vec{\mathcal{P}}\vec{N} & \vec{\mathcal{P}}\vec{A}_\gamma\vec{\mathcal{P}} \end{pmatrix} \begin{pmatrix} \kappa_\gamma^{m+1} \\ \delta\vec{X}^{m+1} \end{pmatrix} = \begin{pmatrix} 0 \\ -\vec{\mathcal{P}}\vec{A}_\gamma\vec{\mathcal{P}}\,\vec{X}^m \end{pmatrix}. \tag{4.8}$$

and

$$\begin{pmatrix} \mathcal{K} A_\beta \mathcal{K} & -\frac{1}{\tau_m} \mathcal{K} \vec{N}^T \vec{\mathcal{P}} \\ \vec{\mathcal{P}} \vec{N} \mathcal{K} & \vec{\mathcal{P}} \vec{A}_\gamma \vec{\mathcal{P}} \end{pmatrix} \begin{pmatrix} \kappa_\gamma^{m+1} \\ \delta \vec{X}^{m+1} \end{pmatrix} = \begin{pmatrix} 0 \\ -\vec{\mathcal{P}} \vec{A}_\gamma \vec{\mathcal{P}} \, \vec{X}^m \end{pmatrix}, \tag{4.9}$$

with the obvious definitions of M_β, A_β and $\vec{A}_\gamma$. Similarly, the schemes (3.10a,b) and (3.11a,b) in the linear case $r = (1, \dots, 1)$ can be formulated as follows. We define the orthogonal projection $\vec{\mathcal{P}}_\partial : (\mathbb{R}^3)^K \to \underline{\mathbb{X}}_\partial$ onto the Euclidean space associated with $\underline{V}_\partial^h(\Gamma^m)$. Then the system (3.11a,b) can be reformulated as: Find $(\delta \vec{X}^{m+1}, \kappa^{m+1}) \in \underline{\mathbb{X}}_\partial \times \mathbb{X}$ such that

$$\begin{pmatrix} \mathcal{K} A_\beta \mathcal{K} & -\frac{1}{\tau_m} \mathcal{K} \vec{N}^T \vec{\mathcal{P}}_\partial \\ \vec{\mathcal{P}}_\partial \vec{N} \mathcal{K} & \vec{\mathcal{P}}_\partial \vec{A}_\gamma \vec{\mathcal{P}}_\partial \end{pmatrix} \begin{pmatrix} \kappa_\gamma^{m+1} \\ \delta \vec{X}^{m+1} \end{pmatrix} = \begin{pmatrix} 0 \\ -\vec{\mathcal{P}}_\partial \vec{A}_\gamma \, \vec{X}^m \end{pmatrix}, \tag{4.10}$$

and similarly for (3.10a,b).

In the truly nonlinear case, i.e. when $r_i > 1$ for some $i = 1 \to I_S$, a lagged fixed point type iteration can be employed, where linear systems of the form e.g. (4.9) need to be solved at each iteration step. See Barrett, Garcke, and Nürnberg (2008c) for analogous details in the case of a single closed hypersurface.

5 Numerical Results

In this section we present several numerical simulations of evolving surface clusters in $\mathbb{R}^3$. We stress that all of the presented experiments were performed without any remeshing. In fact, in practice the initial mesh quality is maintained or even improved on by the intrinsically induced tangential motion of our schemes. A more detailed discussion of this property in the single closed hypersurface case can be found in Barrett, Garcke, and Nürnberg (2008b), while excellent mesh properties for fully anisotropic surface energies in the closed surface case have been presented in Barrett, Garcke, and Nürnberg (2008c).

Throughout this section we use essentially uniform time steps, i.e. $\tau_m = \tau$, $m = 0 \to M-2$, and $\tau_{M-1} = T - t_{m-1}$. For later purposes, we define

$$\vec{X}(t) := \tfrac{t-t_{m-1}}{\tau_{m-1}} \vec{X}^m + \tfrac{t_m - t}{\tau_{m-1}} \vec{X}^{m-1} \qquad t \in [t_{m-1}, t_m] \quad m \geq 1.$$

Finally, we note that we implemented the approximations within the finite element toolbox ALBERTA, see Schmidt and Siebert (2005), where in particular we made use of new submesh tools recently presented in Köster *et al.* (2008).

5.1 Isotropic flows

First we present numerical simulations for isotropic surface energy densities, i.e. $\gamma_i(\vec{p}) = \sigma_i |\vec{p}|$, $\sigma_i > 0$, $i = 1 \to I_S$. Hence the free energy (1.12) reduces to

$$E_\gamma(\Gamma) = \sum_{i=1}^{I_S} \sigma_i |\Gamma_i| . \tag{5.1}$$

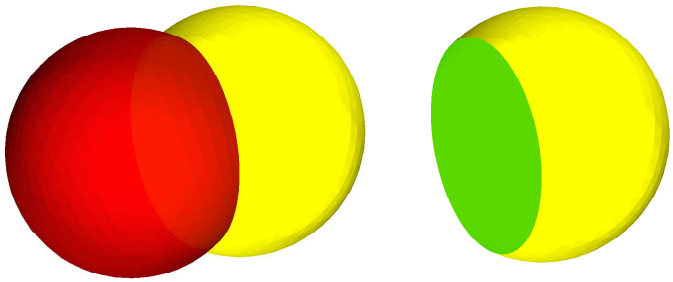

Figure 4: Plots of Γ^M and (Γ_2^M, Γ_3^M).

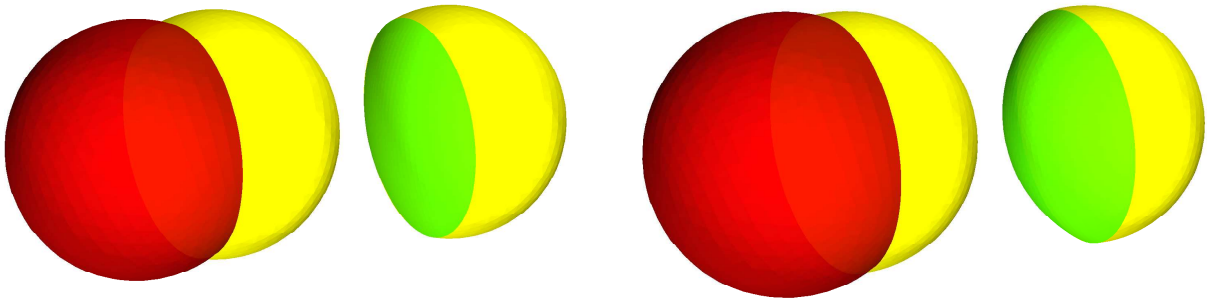

Figure 5: Plots of Γ^M and (Γ_2^M, Γ_3^M) for $\sigma = (1, 1, 1.5)$ (left) and $\sigma = (1, 1, 1.75)$ (right).

Unless otherwise stated, we set $\sigma = (\sigma_1, \ldots, \sigma_{I_S}) = (1, \ldots, 1)$. For the presented computations we employ the schemes (3.10a,b) and (3.11a,b) with $\beta \equiv (1, \ldots, 1)$. Here we recall that in the absence of intersections with an external boundary $\partial\mathcal{D}$ these schemes collapse to (3.7a,b) and (3.8a,b), respectively.

5.1.1 Double bubbles

In the first experiment, we start off with a partition of the unit ball into two half balls. Under the isotropic equal energy density surface diffusion flow this evolves to a standard double bubble, as shown in Figure 4. The discretization parameters for this experiment are $K = 3267$, $J = 6240$, $\tau = 10^{-3}$ and $T = 1$; and the maximum observed relative volume loss was 0.11%; recall Remark 3.1.

In the next experiments, with all other parameters the same as before, we choose $\sigma = (1, 1, 1.5)$ and $\sigma = (1, 1, 1.75)$. The results are in Figure 5. As expected, the higher weighting of the surface area of the surface Γ_3 in the free energy (5.1) leads to this surface shrinking relative to the other two surfaces Γ_1 and Γ_2. The effect becomes more pronounced for larger choices of σ_3.

In addition, we show two experiments for unstable double bubbles, also called torus bubbles; see e.g. Hass and Schlafly (2000, Fig. 7) for an illustration. Here $I_S = 4$ and $I_T = 2$. The initial surface cluster is given by the union of two half spheres and a torus,

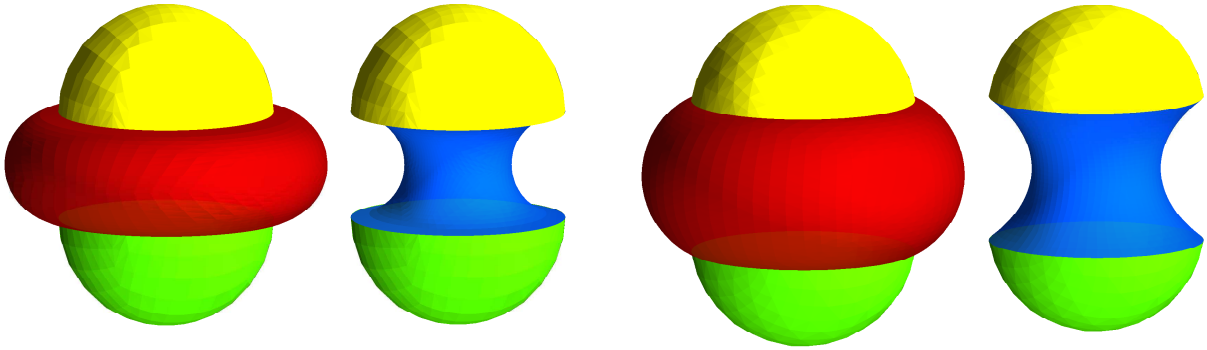

Figure 6: Plots of Γ^m and $(\Gamma_1^m, \Gamma_2^m, \Gamma_4^m)$, $m = 0, M$.

the latter defined by the equation

$$(R - [x_1^2 + x_2^2]^{\frac{1}{2}})^2 + x_3^2 = r^2 \tag{5.2}$$

with $R = 2$ and $r = 1$. Hence the volume relation of the torus/dumbbell volumes is 1.28. The discretization parameters were $K = 4802$, $J = 9216$, $\tau = 10^{-3}$ and $T = 1$. The maximum relative volume loss was 0.08%. See Figure 6 for the results. We note that the final solution at time $T = 1$, which is close to being a numerically steady state, is an approximation of a so called unstable double bubble, which before the proof of the double bubble conjecture was a possible theoretical candidate for a surface area minimizing constellation. Here we recall that the double bubble conjecture states that for two given volumes, the standard double bubble has least possible surface area among all the surfaces enclosing and separating these two volumes. Here the standard double bubble is made up of three constant mean curvature surfaces, meeting along a common circle at an angle of 120 degrees; cf. Figures 4 and 5 for some examples. The conjecture for volumes in $\mathbb{R}^3$ has been proved only relatively recently in Hutchings *et al.* (2002), while the corresponding conjecture for triple bubbles in $\mathbb{R}^3$ still remains open. We refer to the previously mentioned review article Morgan (2007) for more details. In fact, if we continue the simulation in Figure 6 for long enough, then the above mentioned instability becomes evident also in our numerical approximation. As expected, and in agreement with corresponding phase field computations in e.g. Nürnberg (2009, Fig. 13), the inner wall of the torus bubble tries to pinch, which would lead to three separatedly enclosed volumes. These results are shown in Figure 7, together with the corresponding triangulations. Of course, this change of topology goes beyond the parametric formulation employed in this paper and our finite element approximation can only integrate until just before the rupture, which in this case occurs at around time $t = 26.61$. A plot of the free energy $|\Gamma|$ over time can be seen in Figure 8. In addition, we show a simulation for a torus bubble that is not rotationally symmetric, and where the torus part of the double bubble is relatively smaller compared to the previous experiment. Here the initial cluster was obtained by starting with a torus bubble as before, but now in (5.2) setting $R = 2$ and $r = 0.5$, followed by two slight stretchings of this cluster obtained by applying the transformations

$$\mathcal{G}_1(\vec{z}) := \begin{cases} (z_1\, e^{-0.2\, z_1}, z_2, z_3) & z_1 < 0 \\ \vec{z} & z_1 \geq 0 \end{cases} \quad \text{and} \quad \mathcal{G}_2(\vec{z}) := \begin{cases} (z_1, z_2\, e^{-0.1\, z_2}, z_3) & z_2 < 0 \\ \vec{z} & z_2 \geq 0 \end{cases},$$

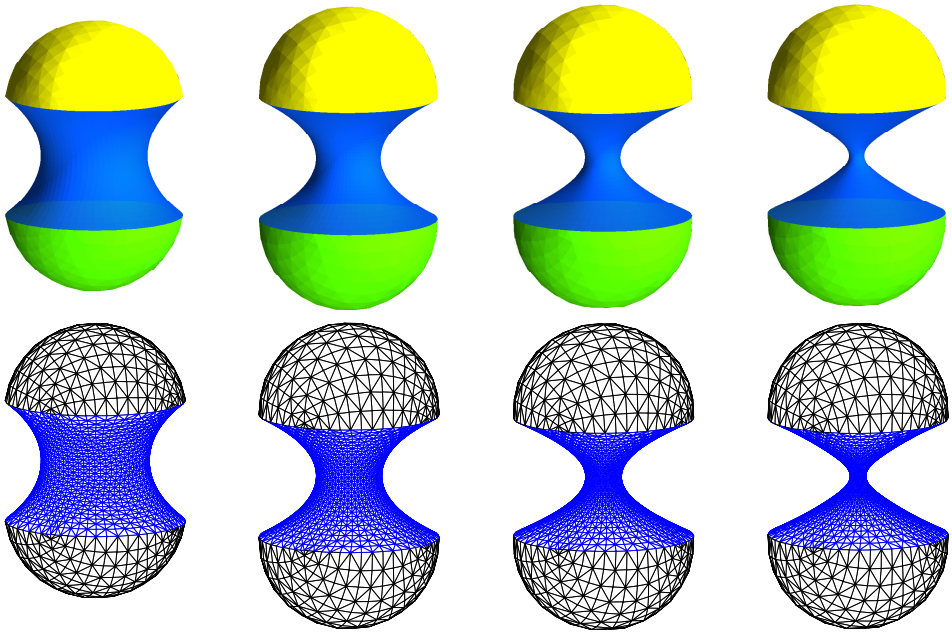

Figure 7: Plots of $(\Gamma_1^m, \Gamma_2^m, \Gamma_4^m)$ at times $t_m = 1$, 25, 26.5, 26.6. Below the corresponding triangulations.

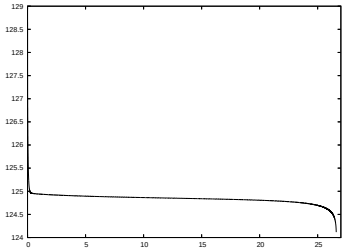

Figure 8: A plot of $|\Gamma|$ over time.

respectively. This resulted in a volume relation of the torus/dumbbell volumes of 0.25. The results of the surface diffusion flow for this torus bubble are shown in Figure 9, where the discretization parameters are $K = 5314$, $J = 10240$ and $\tau = 10^{-3}$. We observe that in this evolution the instability leads to a slightly different behaviour. In particular, it results in the thinning of the toroidal ring at one point. Eventually the thinning would lead to the ring tearing apart, and it appears that this change of topology would occur at around time $t = 0.91$.

5.1.2 Triple bubbles

We first show an experiment for the mean curvature flow. The initial surfaces are given by a partitioning of the unit ball into three equal segments, leading to three curved surfaces and three flat ones, so that $I_S = 6$ and $I_T = 4$. The discretization parameters are $K = 6534$, $J = 12288$, $\tau = 10^{-4}$ and $T = 0.15$. We note that, if continued, the cluster will shrink to a point, as is to be expected for mean curvature flow. In this numerical experiment this happens at around time 0.178. The results are shown in Figure 10.

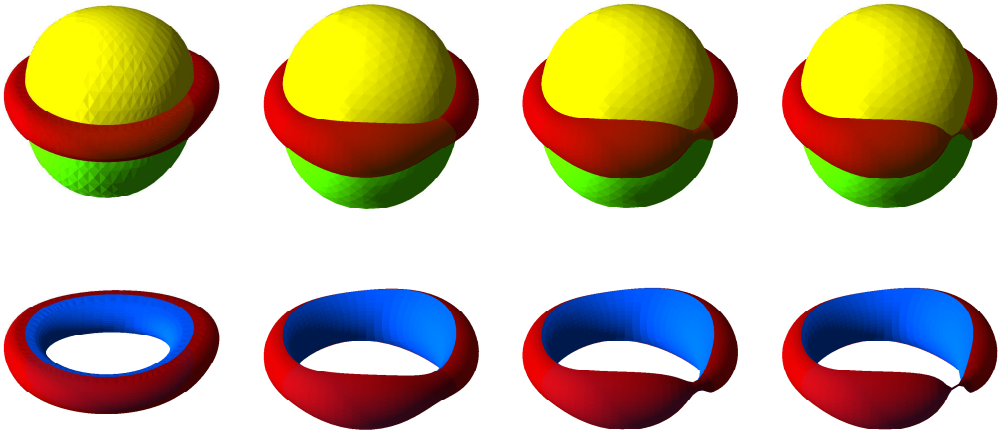

Figure 9: Plots of Γ^m and (Γ_3^m, Γ_4^m) at times $t_m = 0,\ 0.75,\ 0.9,\ 0.91$.

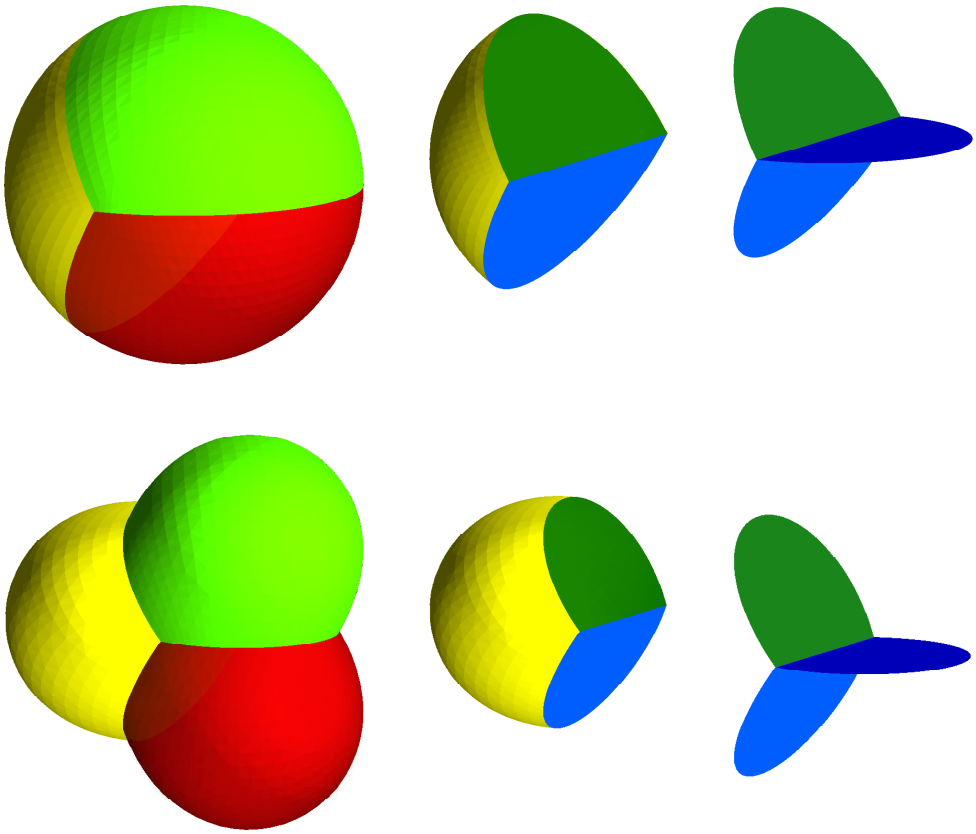

Figure 10: Plots of Γ^m, $(\Gamma_1^m, \Gamma_4^m, \Gamma_5^m)$ and $(\Gamma_4^m, \Gamma_5^m, \Gamma_6^m)$ for $m = 0, M$. (scaled for $m = M$)

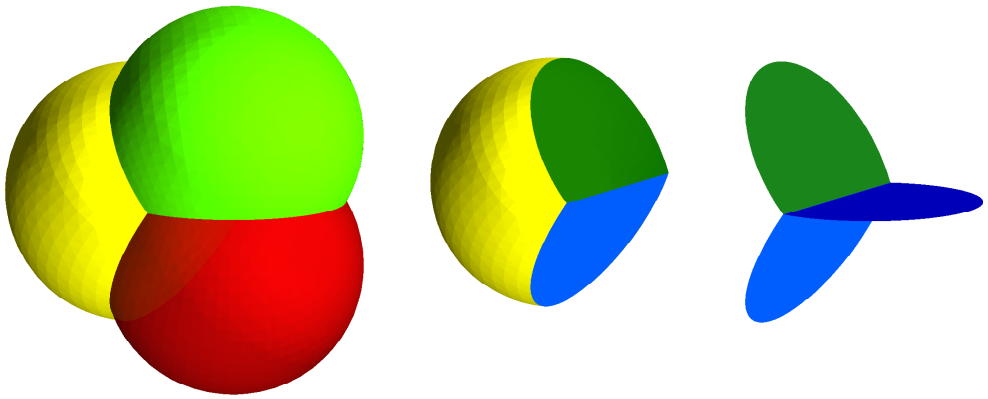

Figure 11: Plots of Γ^M, $(\Gamma_1^M, \Gamma_4^M, \Gamma_5^M)$ and $(\Gamma_4^M, \Gamma_5^M, \Gamma_6^M)$.

We also present computations for a surface diffusion flow. With the same initial surface cluster as before, and the same discretization parameters, we integrate the flow until time $T = 1$. As this stage the solution has reached a numerical steady state, which approximates the well known standard triple bubble. Here we note that the corresponding conjecture that this is indeed the surface area minimizing way to separate three given volumes is still an open problem; although a proof for the planar case has recently been given in Wichiramala (2004). The maximum observed relative volume loss for this computation was 0.03%. See Figure 11 for the results.

In the next experiments, we choose $\sigma = (1.25, 1, 1, 1, 1, 1)$ and $\sigma = (1.5, 1, 1, 1, 1, 1)$. The results are in Figure 12, where the discretization parameters are the same as before. As expected, and similarly to the results shown in Figure 5, we observe that for increasing σ_1 the relative area of the surface Γ_1 shrinks, compared to the remaining surfaces Γ_i, $i = 2 \rightarrow 6$.

5.1.3 Quadruple bubbles

Here we report on an experiment for quadruple bubbles, when four volumes are enclosed by the surface cluster. The cluster consists of $I_S = 9$ surfaces meeting at $I_T = 8$ triple junction lines, which in turn meet at four different quadruple junction points. We start with a configuration made up of two unit cubes and two cuboids, with each cuboid having twice the volume of a unit cube. The discretization parameters were $K = 7305$, $J = 13824$, $\tau = 10^{-4}$ and $T = 1$. The results for the approximation (3.6a,b) can be seen in Figure 13.

5.1.4 Surfaces attached to an external boundary

The first experiment is for a surface that is attached to the boundary of $\mathcal{D} := \mathbb{R}^2 \times (0, \infty)$. Starting with an initial surface in the shape of a unit cube, the surface evolves into a half sphere under flow by surface diffusion, as expected; see the left of Figure 14. The discretization parameters are $K = 5185$, $J = 10240$, $\tau = 10^{-3}$ and $T = 1$. For the

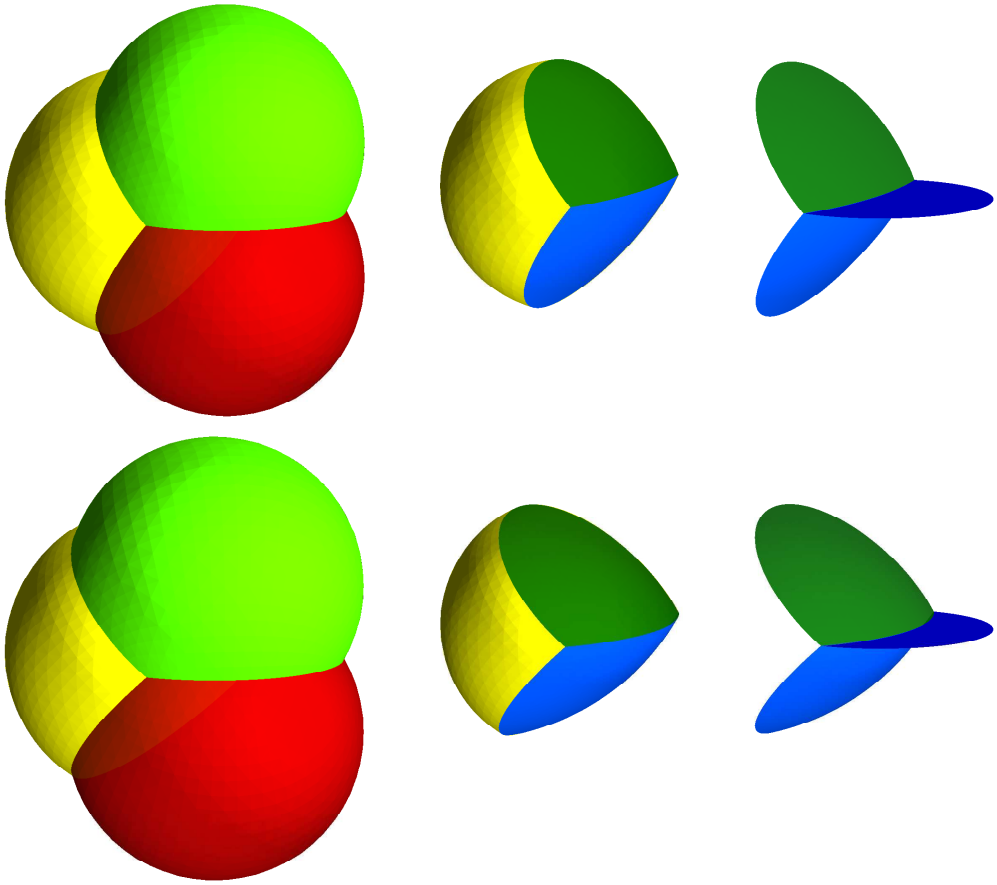

Figure 12: Plots of Γ^M, $(\Gamma_1^M, \Gamma_4^M, \Gamma_5^M)$ and $(\Gamma_4^M, \Gamma_5^M, \Gamma_6^M)$ for $\sigma_1 = 1.25$ (top) and $\sigma_1 = 1.5$ (bottom).

remaining experiments we consider surfaces attached to the lower and upper boundary of the slabs $\mathcal{D} = \mathbb{R}^2 \times (0, \varrho)$, where either $\varrho = 4$ or 8. The surface diffusion flow for the surface defined by

$$\Gamma_1(0) = \bigcup \{ r(x_3)\, S^1 \times \{x_3\} : x_3 \in [0, \varrho] \}\,, \quad \text{where} \quad r(x_3) = 1 + \alpha \cos(\tfrac{2\,\pi\, x_3}{\varrho})\,, \tag{5.3}$$

with $\varrho = 4$ and $\alpha = 0.5$, can be seen on the right of Figure 14, where the discretization parameters are $K = 4160$, $J = 8192$, $\tau = 10^{-3}$ and $T = 2$. This time, we observe that the surface evolves to a cylinder. We note that all of the experiments in this subsection illustrate surface area minimizers for a fixed enclosed volume inside the slabs $\mathcal{D} = \mathbb{R}^2 \times (0, \varrho)$, with $\varrho = 4$ or 8. Here we recall that inside such slab domains the isoperimetric problem is solved, with the surface area minimizing surfaces being either half spheres or cylinders; see e.g. Athanassenas (1987). Finally, in the last two experiments in this subsection we start with two different initial surfaces attached to the boundary of the slab $\mathcal{D} = \mathbb{R}^2 \times (0, 8)$, i.e. $\varrho = 8$. First we start with a triangulation of a cuboid of dimension $1 \times 1 \times 8$ inside $\mathcal{D}$, and this evolves to a cylinder. In fact, as this surface is constant in the x_3-direction the flow is essentially one dimensional, i.e. it corresponds to a square evolving to a circle. However, if we start with a perturbed cylinder inside $\mathcal{D}$, where here we choose (5.3) with $\alpha = 0.25$, then we observe pinch-off and the flow does not

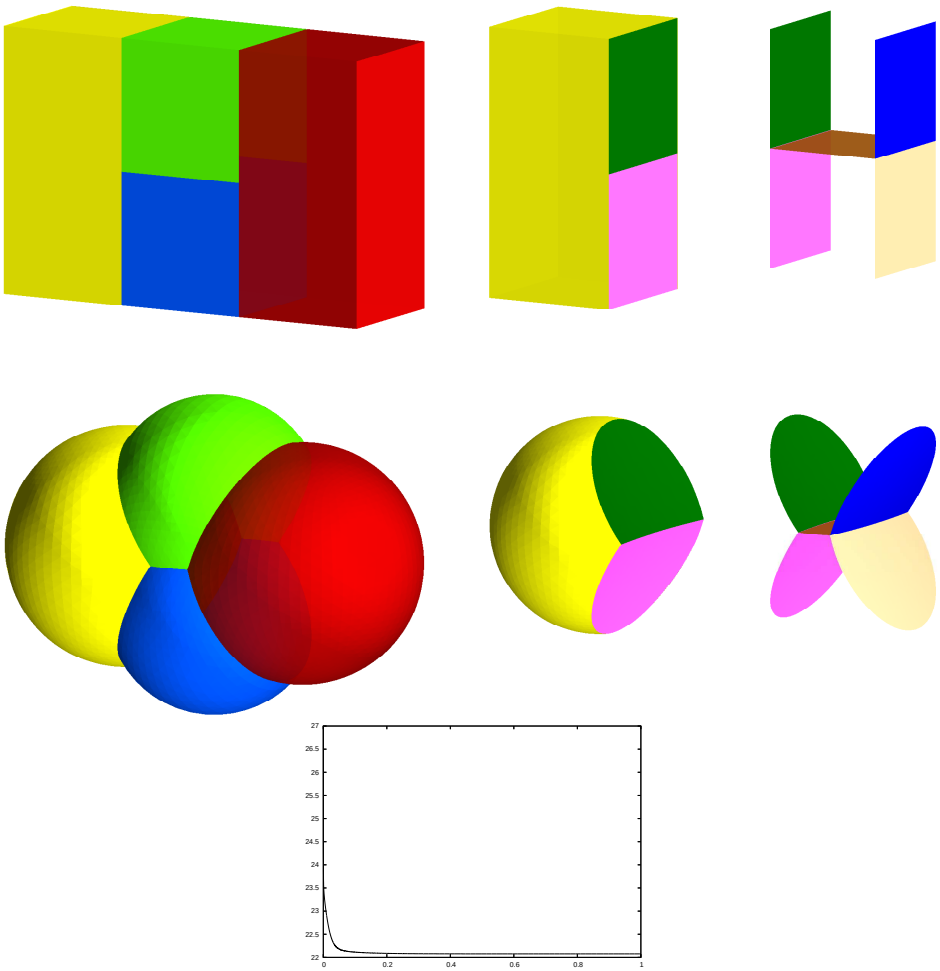

Figure 13: Plots of Γ^m, $(\Gamma_1^m, \Gamma_5^m, \Gamma_7^m)$ and $(\Gamma_5^m, \Gamma_6^m, \Gamma_7^m, \Gamma_8^m, \Gamma_9^m)$ for $m = 0, M$. Below a plot of $|\Gamma|$ over time.

Figure 14: Plots of Γ^0 and Γ^M.

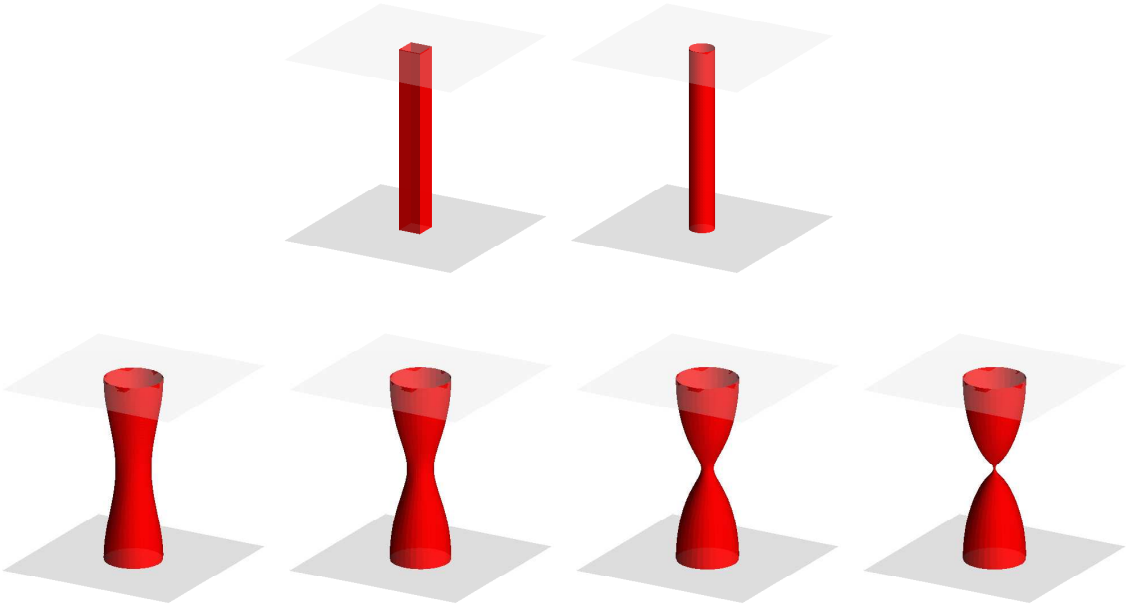

Figure 15: Plots of Γ^0 and Γ^M (top) and plots of Γ^m for $t_m = 0$, 1, 1.45, 1.48 (bottom).

converge to a cylinder, which in this case is unstable; see Athanassenas (1987). Instead, the flow wants to separate the surface into two surfaces, which would each evolve into a half sphere. Of course, as mentioned before, such a change of topology is beyond the parametric formulation and hence, without a heuristically defined reparameterization, our finite element approximation can only integrate until just before the pinch-off, which in this case occurs at around time $t = 1.487$. The discretization parameters are $K = 4128$, $J = 8192$, $\tau = 10^{-3}$, and the results can be seen in Figure 15.

5.2 Anisotropic flows

In what follows we present numerical results for fully anisotropic evolution equations for surface clusters. Here we employ our schemes (3.10a,b) and (3.11a,b), where we recall that in the absence of intersections with an external boundary $\partial\mathcal{D}$ these schemes collapse to (3.7a,b) and (3.8a,b), respectively.

Unless otherwise stated, we choose the constant mobility $\beta = (1, \dots, 1)$ and set $\gamma = (\gamma_1, \dots, \gamma_1)$, where γ_1 is chosen of the form (1.15) with (1.17).

5.2.1 Anisotropic mean curvature flow

Similarly to Soner (1993), it can be proven that for an anisotropy that is symmetric with respect to the x_3-axis and for the anisotropic mobility $\beta = \gamma$, an exact solution to (1.19) with $I_S = 1$ for a single hypersurface touching the boundary of $\mathcal{D} := \mathbb{R}^2 \times (0, \infty)$ is given by

$$\Gamma(t) = \{\vec{q} \in \mathbb{R}^3 : \gamma_1^*(\vec{q}) = \sqrt{1 - 4\,t}\} \cap \overline{\mathcal{D}}\,, \tag{5.4}$$

Table 1: Absolute errors $\|\vec{X}-\vec{x}\|_{L^\infty}$ for the test problem, with $T=\frac{1}{2}\,\overline{T}=\frac{1}{8}$ and $T=\overline{T}-\tau$, respectively.

K	$\varepsilon_1=0.5$			$\varepsilon_1=0.1$		
	$h_{\vec{X}^0}$	$T=\frac{1}{2}\,\overline{T}$	$T=\overline{T}-\tau$	$h_{\vec{X}^0}$	$T=\frac{1}{2}\,\overline{T}$	$T=\overline{T}-\tau$
289	2.7470e-01	7.8899e-03	1.0094e-01	2.7076e-01	4.6355e-03	1.0020e-01
1089	1.3957e-01	2.2296e-03	7.6033e-02	1.3801e-01	1.5169e-03	7.6160e-02
4225	7.0067e-02	5.8183e-04	4.9572e-02	6.9339e-02	4.0686e-04	4.9487e-02
16641	3.5069e-02	1.5238e-04	3.0130e-02	3.4711e-02	1.2193e-04	3.4094e-02

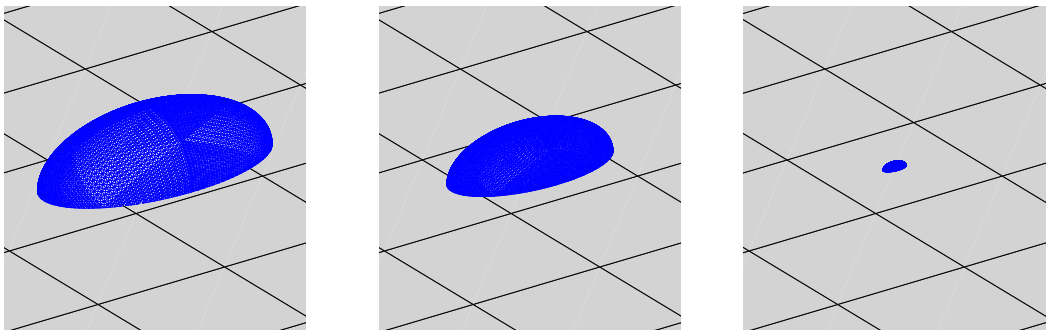

Figure 16: Plots of $\vec{X}(t)$ at times $t=0,\ \frac{1}{2}\bar{T},\ \bar{T}-\tau$.

i.e. shrinking (upper) halves of boundaries of Wulff shapes, recall (1.16). Using (5.4) we now perform a convergence test for our approximation (3.10a,b) with $\beta=\gamma$. An exact solution to (1.19) with $I_S=1$ and $\beta=\gamma$ defined by (1.15) with $L_1=1$ and $G_1^{(1)}=\mathrm{diag}(1,\varepsilon_1^2,\varepsilon_1^2)$, on noting (1.16) and (5.4), is given by

$$\vec{x}_1(\cdot,t)=(1-4\,t)^{\frac{1}{2}}\,[G_1^{(1)}]^{\frac{1}{2}}\,\vec{\mathrm{id}}_{S^2_{\geq 0}},\quad t\in[0,\overline{T}),\quad \overline{T}=0.25\,; \tag{5.5}$$

where $\vec{\mathrm{id}}_{S^2_{\geq 0}}$ is the identity function on the upper unit sphere $\Omega\equiv S^2_{\geq 0}\subset\mathbb{R}^3$. For $\varepsilon_1=0.5$ and $\varepsilon_1=0.1$ we report on the error $\|\vec{X}-\vec{x}\|_{L^\infty}$ in Table 1. Here we always compute the error $\|\vec{X}-\vec{x}\|_{L^\infty}:=\max_{m=1\to M}\|\vec{X}(t_m)-\vec{x}(\cdot,t_m)\|_{L^\infty}$, where $\|\vec{X}(t_m)-\vec{x}(\cdot,t_m)\|_{L^\infty}:=\max_{k=1\to K_1}\left\{\min_{\vec{y}\in\Omega}|\vec{X}_1^m(\vec{q}_k^{\,1})-\vec{x}_1(\vec{y},t_m)|\right\}$ between $\vec{X}$ and the true solution on the interval $[0,T]$ by employing a Newton method. We used $\tau=0.125\,h^2_{\vec{X}^0}$ and either $T=\frac{1}{2}\,\overline{T}$ o $T=\overline{T}-\tau$, where $h_{\vec{X}^0}:=\max_{i=1\to I_S}\max_{j=1\to J_i}\mathrm{diam}(\vec{X}_i^0(\sigma_j^i))$. We note that the experiments indicate that the convergence rate for the error away from the singularity is $O(h^2)$, and up to the singularity at time $\overline{T}$ is of order less than $O(h)$, which corresponds to the results obtained for the closed hypersurface case in Barrett, Garcke, and Nürnberg (2008c). In Figure 16, we present the evolution for the case $K=4225$ and $\varepsilon_1=0.5$. We note that for the convergence experiments in Table 1 the condition (3.12) was satisfied exactly throughout. As noted earlier, in this case this is to be expected since $\partial\mathcal{D}$ is flat.

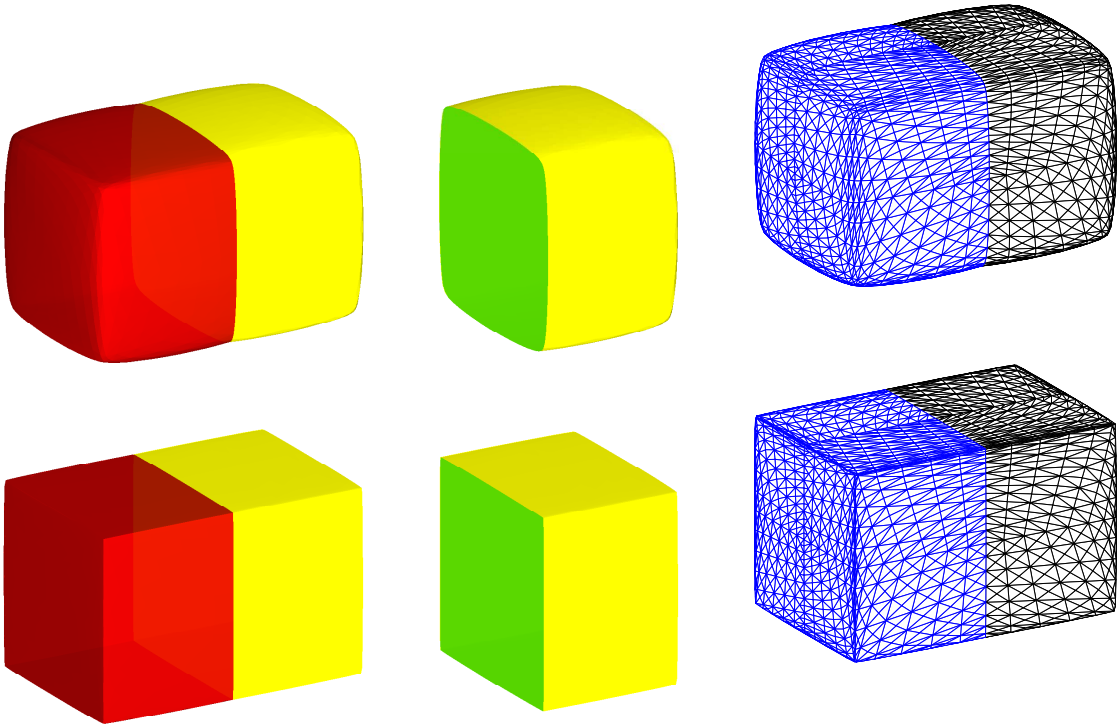

Figure 17: Plots of Γ^M, (Γ_2^M, Γ_3^M) and the triangulations of Γ^M for $\varepsilon_1 = 10^{-1}$ (top) and $\varepsilon_1 = 10^{-2}$ (bottom).

5.2.2 Anisotropic surface diffusion

For the anisotropy as displayed on the left of Figure 2, i.e. for the regularized l^1-norm

$$\gamma_1(\vec{p}) = \sum_{j=1}^{3} \left[\varepsilon_1^2 \, |\vec{p}|^2 + p_j^2 \, (1 - \varepsilon_1^2)\right]^{\frac{1}{2}} , \tag{5.6}$$

we repeat the experiment in Figure 4, now for the anisotropic flow. Here we choose $\varepsilon_1 = 10^{-1}$ and $\varepsilon_1 = 10^{-2}$ in (5.6). The discretization parameters for the two experiments are $K = 3267$, $J = 6240$ and $\tau = 10^{-3}$, $T = 1$. See Figure 17 for the results, where we note once again that our scheme produces good quality meshes throughout. In addition, we observe that our finite element approximation can easily handle these almost crystalline surface energies, which suggests that it can be used to numerically study possible energy minimizing configurations of e.g. salt crystals, as discussed in e.g. Morgan *et al.* (1998); Wecht *et al.* (2000).

Moreover, we repeated the experiment in Figure 17 but used an isotropic surface energy density $\gamma_2 = \gamma_3 = |\cdot|$ for the surfaces Γ_2 and Γ_3, while γ_1 is given by (5.6) with $\varepsilon_1 = 10^{-2}$. The numerical results for this simulation are shown in Figure 18.

The next experiment is for the setup as in Figure 11, but now for the anisotropic surface energy densities γ_i all chosen as on the right of Figure 2. With the same discretization parameters as in Figure 11, we obtained the results as displayed in Figure 19.

In the remainder, we present some computations for the anisotropic surface diffusion

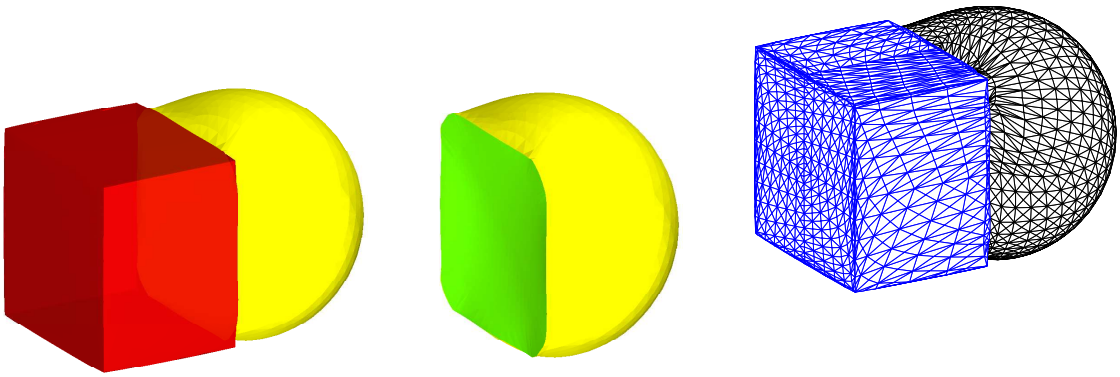

Figure 18: Plots of Γ^M, (Γ_2^M, Γ_3^M) and the triangulations of Γ^M.

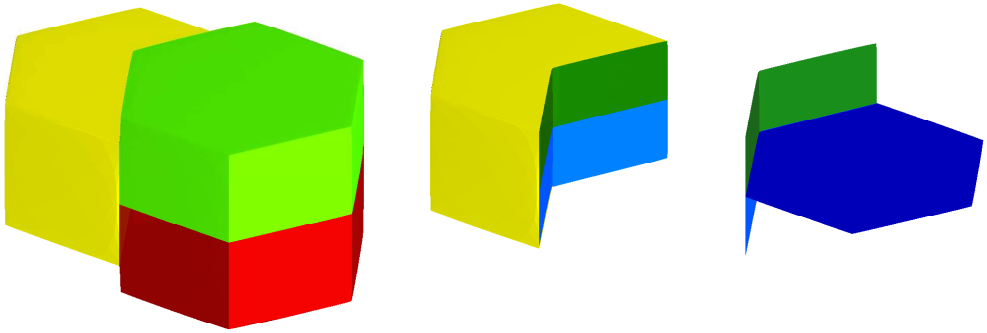

Figure 19: Plots of Γ^M, $(\Gamma_1^M, \Gamma_4^M, \Gamma_5^M)$ and $(\Gamma_4^M, \Gamma_5^M, \Gamma_6^M)$.

flow of a single surface attached to the boundary of $\mathcal{D} := \{\vec{q} \in \mathbb{R}^3 : q_3 > 0\}$. As initial surface we choose a unit half sphere attached to $\partial\mathcal{D}$. The discretization parameters are $K = 4225$, $J = 8256$, $\tau = 10^{-3}$ and $T = 1$. The results for the choices $\gamma_1(\vec{p}) = |\vec{p}|$, as well as the two anisotropies displayed in Figure 3 are shown in Figure 20. As expected, the initial surfaces evolve to upper halves of Wulff shapes. We note that the last example has clear resemblances with shapes observed in the laboratory for epitaxial thin film growth, see e.g. Venables (2000, Fig. 5.12). We also remark that in epitaxial thin film growth the equilibrium state is given as a stationary solution of an anisotropic surface energy and that surface diffusion is the main transport mechanism in this context. Hence the flow (1.20) is a relevant equation for surface evolution in thin film growth, although more general models take elastic effects into account, see e.g. Gurtin and Jabbour (2002).

References

Almgren, F. and Taylor, J. E. (1996). Soap bubble clusters. *Forma*, **11**(3), 199–207.

Almgren, Jr., F. J. (1976). Existence and regularity almost everywhere of solutions to elliptic variational problems with constraints. *Mem. Amer. Math. Soc.*, **4**(165), viii+199.

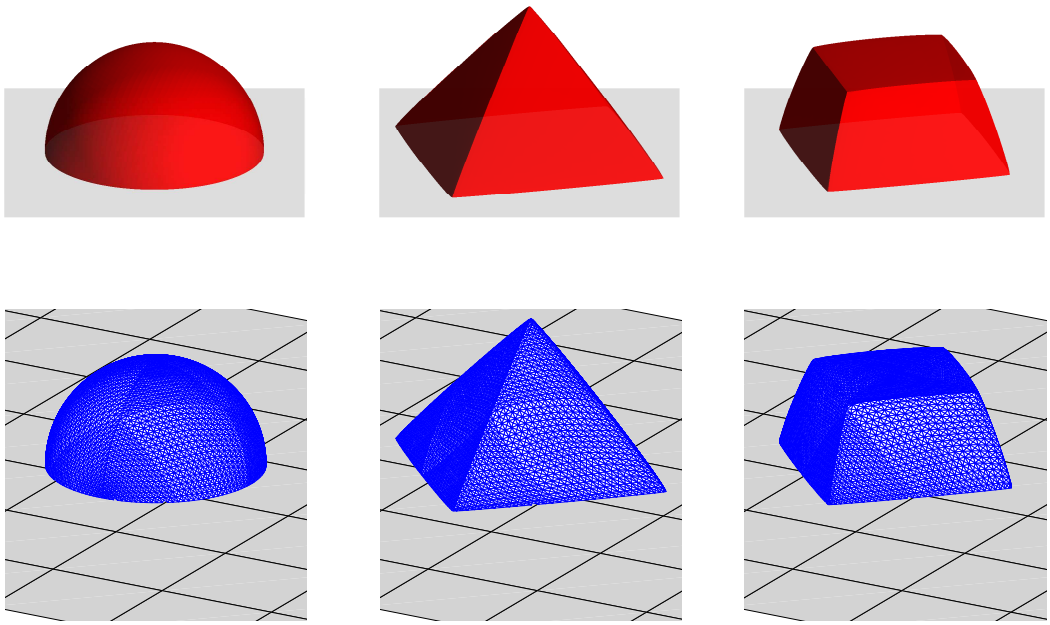

Figure 20: Plots of $\vec{X}^M$ for different anisotropies, with the triangulations given below.

Angenent, S. and Gurtin, M. E. (1989). Multiphase thermomechanics with interfacial structure. II. Evolution of an isothermal interface. *Arch. Rational Mech. Anal.*, **108**(4), 323–391.

Athanassenas, M. (1987). A variational problem for constant mean curvature surfaces with free boundary. *J. Reine Angew. Math.*, **377**, 97–107.

Barrett, J. W., Garcke, H., and Nürnberg, R. (2007a). A parametric finite element method for fourth order geometric evolution equations. *J. Comput. Phys.*, **222**(1), 441–467.

Barrett, J. W., Garcke, H., and Nürnberg, R. (2007b). On the variational approximation of combined second and fourth order geometric evolution equations. *SIAM J. Sci. Comput.*, **29**(3), 1006–1041.

Barrett, J. W., Garcke, H., and Nürnberg, R. (2007c). A phase field model for the electromigration of intergranular voids. *Interfaces Free Bound.*, **9**(2), 171–210.

Barrett, J. W., Garcke, H., and Nürnberg, R. (2008a). Numerical approximation of anisotropic geometric evolution equations in the plane. *IMA J. Numer. Anal.*, **28**(2), 292–330.

Barrett, J. W., Garcke, H., and Nürnberg, R. (2008b). On the parametric finite element approximation of evolving hypersurfaces in $\mathbb{R}^3$. *J. Comput. Phys.*, **227**(9), 4281–4307.

Barrett, J. W., Garcke, H., and Nürnberg, R. (2008c). A variational formulation of anisotropic geometric evolution equations in higher dimensions. *Numer. Math.*, **109**(1), 1–44.

Barrett, J. W., Garcke, H., and Nürnberg, R. (2009). Finite element approximation of a phase field model for multicomponent surface diffusion. (in preparation).

Betounes, D. E. (1986). Kinematics of submanifolds and the mean curvature normal. *Arch. Rational Mech. Anal.*, **96**(1), 1–27.

Brakke, K. A. (1978). *The motion of a surface by its mean curvature*, volume 20 of *Mathematical Notes*. Princeton University Press, Princeton, N.J.

Brakke, K. A. (1992). The surface evolver. *Experiment. Math.*, **1**(2), 141–165.

Bronsard, L. and Reitich, F. (1993). On three-phase boundary motion and the singular limit of a vector-valued Ginzburg-Landau equation. *Arch. Rational Mech. Anal.*, **124**(4), 355–379.

Bronsard, L., Garcke, H., and Stoth, B. (1998). A multi-phase Mullins-Sekerka system: matched asymptotic expansions and an implicit time discretisation for the geometric evolution problem. *Proc. Roy. Soc. Edinburgh Sect. A*, **128**(3), 481–506.

Cahn, J. W. (1991). Stability, microstructural evolution, grain growth, and coarsening in a two-dimensional two-phase microstructure. *Acta Metall.*, **39**, 2189–2199.

Cahn, J. W. and Hoffmann, D. W. (1974). A vector thermodynamics for anisotropic surfaces – II. curved and faceted surfaces. *Acta Metall.*, **22**, 1205–1214.

Cahn, J. W., Holm, E. A., and Srolovitz, D. J. (1992). Modeling microstructural evolution in two-dimensional two-phase microstructures. *Mater. Sci. Forum*, **94–96**, 141–158.

Cox, S. J. and Graner, F. (2004). Three-dimensional bubble clusters: Shape, packing, and growth rate. *Phys. Rev. E*, **69**(3), 031409.

Deckelnick, K., Dziuk, G., and Elliott, C. M. (2003). Error analysis of a semidiscrete numerical scheme for diffusion in axially symmetric surfaces. *SIAM J. Numer. Anal.*, **41**(6), 2161–2179.

Depner, D., Garcke, H., and Kohsaka, Y. (2009). Mean curvature flow of surface clusters. (in preparation).

Dziuk, G. (1991). An algorithm for evolutionary surfaces. *Numer. Math.*, **58**(6), 603–611.

Dziuk, G. (1994). Convergence of a semi-discrete scheme for the curve shortening flow. *Math. Models Methods Appl. Sci.*, **4**, 589–606.

Foisy, J., Alfaro, M., Brock, J., Hodges, N., and Zimba, J. (1993). The standard double soap bubble in $\mathbb{R}^2$ uniquely minimizes perimeter. *Pacific J. Math.*, **159**(1), 47–59.

Fonseca, I. and Müller, S. (1991). A uniqueness proof for the Wulff theorem. *Proc. Roy. Soc. Edinburgh Sect. A*, **119**(1-2), 125–136.

Garcke, H. and Nestler, B. (2000). A mathematical model for grain growth in thin metallic films. *Math. Models Methods Appl. Sci.*, **10**, 895–921.

Garcke, H. and Novick-Cohen, A. (2000). A singular limit for a system of degenerate Cahn-Hilliard equations. *Adv. Differential Equations*, **5**(4-6), 401–434.

Garcke, H. and Wieland, S. (2006). Surfactant spreading on thin viscous films: nonnegative solutions of a coupled degenerate system. *SIAM J. Math. Anal.*, **37**(6), 2025–2048.

Garcke, H., Nestler, B., and Stoth, B. (1999). A multiphase field concept: numerical simulations of moving phase boundaries and multiple junctions. *SIAM J. Appl. Math.*, **60**(1), 295–315.

Garcke, H., Nestler, B., Stinner, B., and Wendler, F. (2008). Allen–Cahn systems with volume constraints. *Math. Models Methods Appl. Sci.*, **18**(8), 1347–1381.

Gurtin, M. E. (1993). *Thermomechanics of evolving phase boundaries in the plane*. Oxford Mathematical Monographs. The Clarendon Press Oxford University Press, New York.

Gurtin, M. E. (2000). *Configurational forces as basic concepts of continuum physics*, volume 137 of *Applied Mathematical Sciences*. Springer-Verlag, New York.

Gurtin, M. E. and Jabbour, M. E. (2002). Interface evolution in three dimensions with curvature-dependent energy and surface diffusion: interface-controlled evolution, phase transitions, epitaxial growth of elastic films. *Arch. Ration. Mech. Anal.*, **163**(3), 171–208.

Hass, J. and Schlafly, R. (2000). Double bubbles minimize. *Ann. of Math. (2)*, **151**(2), 459–515.

Hass, J., Hutchings, M., and Schlafly, R. (1995). The double bubble conjecture. *Electron. Res. Announc. Amer. Math. Soc.*, **1**(3), 98–102.

Herring, C. (1951). Surface tension as a motivation for sintering. In W. E. Kingston, editor, *The Physics of Powder Metallurgy*, pages 143–179. McGraw–Hill, New York.

Hestenes, M. R. (1975). Pseudoinverses and conjugate gradients. *Comm. ACM*, **18**, 40–43.

Hildebrandt, S. and Tromba, A. (1985). *Mathematics and optimal form*. Scientific American Library, New York.

Hutchings, M., Morgan, F., Ritoré, M., and Ros, A. (2002). Proof of the double bubble conjecture. *Ann. of Math. (2)*, **155**(2), 459–489.

Köster, D., Kriessl, O., and Siebert, K. G. (2008). Design of finite element tools for coupled surface and volume meshes. *Numer. Math. Theory Methods Appl.*, **1**(3), 245–274.

Kraynik, A. M., Reinelt, D. A., and van Swol, F. (2004). Structure of random foam. *Phys. Rev. Lett.*, **93**(20), 208301.

Lawlor, G. and Morgan, F. (1994). Paired calibrations applied to soap films, immiscible fluids, and surfaces or networks minimizing other norms. *Pacific J. Math.*, **166**(1), 55–83.

Morgan, F. (1988). *Geometric Measure Theory: a Beginner's Guide*. Academic Press Inc., Boston, MA.

Morgan, F. (1994). Soap bubbles in $\mathbb{R}^2$ and in surfaces. *Pacific J. Math.*, **165**(2), 347–361.

Morgan, F. (2007). Colloquium: Soap bubble clusters. *Rev. Modern Phys.*, **79**(3), 821–827.

Morgan, F., French, C., and Greenleaf, S. (1998). Wulff clusters in $\mathbb{R}^2$. *J. Geom. Anal.*, **8**(1), 97–115.

Mullins, W. W. (1956). Two dimensional motion of idealized grain boundaries. *J. Appl. Phys.*, **27**, 900–904.

Mullins, W. W. (1958). The effect of thermal grooving on grain boundary motion. *Acta Metall.*, **6**, 414–427.

Nestler, B., Wendler, F., Selzer, M., Stinner, B., and Garcke, H. (2008). Phase-field model for multiphase systems with preserved volume fractions. *Phys. Rev. E*, **78**, 011604.

Nürnberg, R. (2009). Numerical simulations of immiscible fluid clusters. *Appl. Numer. Math.* `doi:10.1016/j.apnum.2008.11.003`, (to appear).

Pozzi, P. (2008). Anisotropic mean curvature flow for two dimensional surfaces in higher codimension: a numerical scheme. *Interfaces Free Bound.*, **10**(4), 539–576.

Schmidt, A. and Siebert, K. G. (2005). *Design of Adaptive Finite Element Software: The Finite Element Toolbox ALBERTA*, volume 42 of *Lecture Notes in Computational Science and Engineering*. Springer-Verlag, Berlin.

Smith, C. S. (1948). Grains, phases, and interfaces: an interpretation of microstructure. *Trans. Am. Inst. Mining Met. Eng.*, **175**, 15–51.

Soner, H. M. (1993). Motion of a set by the curvature of its boundary. *J. Differential Equations*, **101**(2), 313–372.

Sullivan, J. M. and Morgan, F. (1996). Open problems in soap bubble geometry. *Internat. J. Math.*, **7**(6), 833–842.

Sutton, A. P. and Balluffi, R. W. (1995). *Interfaces in Crystalline Materials*. Clarendon Press, Oxford.

Taylor, J. E. (1976). The structure of singularities in soap-bubble-like and soap-film-like minimal surfaces. *Ann. of Math. (2)*, **103**(3), 489–539.

Taylor, J. E. (1999). Mathematical models of triple junctions. *Interface Sci.*, **7**(3-4), 243–249.

Taylor, J. E. and Cahn, J. W. (1994). Linking anisotropic sharp and diffuse surface motion laws via gradient flows. *J. Statist. Phys.*, **77**(1-2), 183–197.

Taylor, J. E., Cahn, J. W., and Handwerker, C. A. (1992). Geometric models of crystal growth. *Acta Metall. Mater.*, **40**, 1443–1474.

Venables, J. A. (2000). *Introduction to Surface and Thin Film Processes*. Cambridge University Press, Cambridge.

Wecht, B., Barber, M., and Tice, J. (2000). Double crystals. *Acta Cryst. Sect. A*, **56**(1), 92–95.

Wichiramala, W. (2004). Proof of the planar triple bubble conjecture. *J. Reine Angew. Math.*, **567**, 1–49.

Wulff, G. (1901). Zur Frage der Geschwindigkeit des Wachstums und der Auflösung der Kristallflächen. *Z. Krist.*, **34**, 449–530.

Zhao, H.-K., Merriman, B., Osher, S., and Wang, L. (1998). Capturing the behavior of bubbles and drops using the variational level set approach. *J. Comput. Phys.*, **143**(2), 495–518.